MASTER

~~CONFIDENTIAL~~
~~RESTRICTED DATA~~
~~Atomic Energy Act - 1954~~

NOTICE

This report was prepared as an account of work sponsored by the United States Government. Neither the United States nor the United States Energy Research and Development Administration, nor any of their employees, nor any of their contractors, subcontractors, or their employees, makes any warranty, express or implied, or assumes any legal liability or responsibility for the accuracy, completeness or usefulness of any information, apparatus, product or process disclosed, or represents that its use would not infringe privately owned rights.

December 1965

Westinghouse Astronuclear Laboratory

~~INFORMATION CATEGORY~~
~~CONFIDENTIAL - RD~~
~~AUTHORIZED CLASSIFIER~~ ~~DATE~~

[redacted]

Prepared by:
Test Engineering

1 7624

Approved by:

J. B. Mc Guffin, Mgr.
Test Engineering

G. R. Thomas, Mgr.
Nuclear Systems Eng

WANL-TNR-210

NPX-A3
Final Report

(Title Unclassified)

Subcontract NP-1

~~THIS IS~~ A NERVA RESEARCH AND ~~DEVELOPMENT~~ REPORT AND ~~IS DISTRIBUTED~~ TO ALL ~~AEC~~ C-91 ADDRESSES.

~~CONFIDENTIAL~~
~~RESTRICTED DATA~~
~~Atomic Energy Act - 1954~~

BLANK PAGE

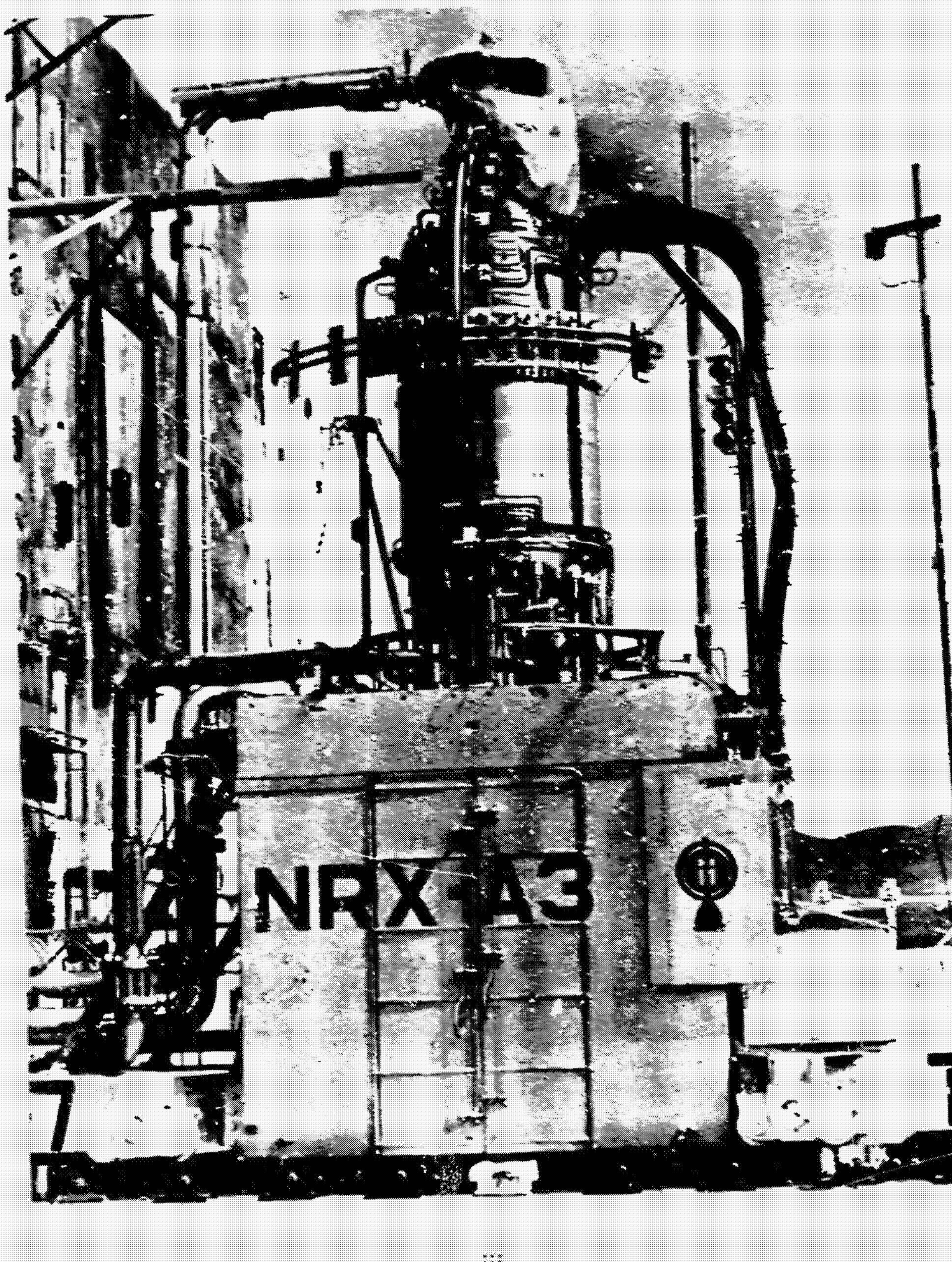
NRX-A3

BLANK PAGE

ACKNOWLEDGEMENTS

The material presented in this report represents contributions from members of several organizations--the Space Nuclear Propulsion Office (SNPO), Aerojet-General Corporation (AGC), NERVA Test Operations (NTO), as well as the Westinghouse Astronuclear Laboratory (WANL). At WANL, specific sections of this report were prepared by various departments--Reactor Analysis, Reactor Mechanical Design, Materials, Systems Integration, Instrumentation and Control, and Test Engineering--and full credit is extended to these groups for their participation. The references enumerated in the bibliography of this report will provide more comprehensive information in specific areas of interest.

BLANK PAGE

Astronuclear Laboratory

WANL-TNR-210

NRX-A3 FINAL REPORT

TABLE OF CONTENTS

I. INTRODUCTION

A. NERVA PROGRAM

As the name implies, the overall objective of the NERVA (Nuclear Engine for Rocket Vehicle Applications) program is the development of a solid-core nuclear reactor-powered flight engine for space vehicles. The specific impulse advantages of such a system over chemical-powered rockets, especially in the upper-stages of an interplanetary mission vehicle, have been well documented in other places and require no discussion here. The NERVA program, which is currently in progress, is a continuation and extension of the KIWI series of tests performed by the Los Alamos Scientific Laboratory. Both the KIWI tests and the present NERVA tests utilize the test facilities at the Nuclear Rocket Development Station (NRDS) at Jackass Flats, Nevada.

Specifically, the objectives of the NERVA program are as follows:

1) Design and develop a solid-core nuclear reactor for use in technology development which may later be applied to a flight engine.

2) Demonstrate the feasibility of the reactor and engine operation through ground testing phases.

3) Develop the necessary facilities, logistics planning, and experienced personnel for performance of the NERVA program and as a basis for future phases.

B. SUMMARY OF PREVIOUS REACTOR TESTS

The reactor tests performed to date in the NERVA development program are the NRX-A1 cold flow test series (unfueled graphite core, Reference 1), the NRX-A2 power test series (Reference 2), and the NRX-A3 power test series, the results of which are presented in this report. In addition, the NRX-A1 reactor assembly is being used in the Cold Flow Development Test System (CFDTS), for studies of the hot-bleed, or "bootstrap", system in nuclear rocket engine design (Reference 3).

The primary objectives of each of the above tests have been achieved and were as follows:

1 NRX-A1

a) Verify reactor structural integrity under full pressure drop loadings

b) Obtain reactor performance data under ambient and cold flow conditions.

2 NRX-A2

a) To provide significant information for verifying the steady-state design analysis for power operation

b) To provide significant information which will aid in assessing the suitability of the reactor to operate at the steady-state power level and temperatures required for the reactor to be a component of an experimental engine system.

3 NRX-A3

a) To operate at full power for fifteen minutes with margin for operation at full power for a period of five minutes after restart.

b) To shut down and cool down on liquid hydrogen.

c) To start up from a low-power low-flow steady-state operating condition and to shut down from a medium power level on liquid hydrogen flow control only.

d) To check the stability of certain new control concepts.

e) To determine the acceptability of design changes and modifications to this test article.

f) To verify the limits of the predicted steady-state power flow operating map up to medium power.

4 CFDTS

a) Evaluate the effect of system paramerers during early stages of "bootstrap" startup of future tests, i.e., NRX/EST and XE-engine (flight-configuration down-firing engine) tests.

b) Obtain closed-cycle system performance data under ambient and cold flow conditions.

During the NRX-A1 tests, there was no evidence of large, low frequency vibrations (which had occurred in the KIWI reactor series), either forced or self-excited, which would imply possible dynamic instability in the reactor assembly. The absence of these vibrations verified the adequacy of the design of the core support structure. Post-operative examination revealed few signs of the effects of testing on the reactor components.

The NRX-A2 reactor was operated for seven minutes at an average power level of 813 megawatts. The liquid hydrogen flow rate averaged 75.6 ± 1.5 lb/sec. During the seven minutes the power reached 1096 ± 50 megawatts for 40 seconds, which verified the ability of the reactor and nozzle to withstand the environment at full power. The specific impulse at the full-power hold was 745 ± 18 seconds (corrected to vacuum), and the thrust was 55,500 pounds. During the test series reactor stability was demonstrated with constant control drum position for propellant flow rates between 5.2 and 13.5 lb/sec in the power range of 2.0 to 4.7 percent of full power (1120 megawatts). The fixed control drum test demonstrated the feasibility of controlling the reactor on propellant flow only. Another test was performed with flow rates between 8.3 and 13.5 lb/sec on dewar pressure alone (no pump operating) at a constant 3.4 percent of full power.

Overall fuel and graphite component behavior was generally as expected. However, as a result of observed corrosion in certain discrete areas, design changes were made in the NRX-A3 to prolong fuel and graphite endurance.

BLANK PAGE

II. SUMMARY

The NRX-A3 test series was completed in May 1965, at the Nuclear Rocket Development Station (NRDS). The test series was comprised of seven experimental plans (EP's), which were intended to bring the NRX-A3 in a series of low-flow, low-power tests to a full design power test. During EP-IV, after 3.5 minutes of full power (1120 megawatt) operation, an unplanned automatic shutdown occurred, which subsequently resulted in overheating of the core tie rod assembly. It is believed that a loose electrical connection in the turbine overspeed circuit was the cause of this shutdown. A comprehensive review of all the test data indicated that the reactor was not damaged, and a decision was made to continue the tests with a full power restart.

During EP-V, the reactor was operated for 16 minutes, 13.1 minutes of which were at full power. The total integrated operating times for EP-IV and EP-V was 22 minutes, with 16.6 minutes at full power. The specific impulse achieved at the full power hold was approximately 750 seconds, corrected to vacuum conditions, while the calculated thrust was 53,400 pounds.

The reactor was started a third time during EP-VI primarily for medium power mapping and controls tests. A significant feature of these tests was a fixed control drum position test in which the reactor power was controlled with the propellant flow rate only. The results were in excellent agreement with the predictions. This test showed definitely that the reactor is inherently stable on liquid hydrogen flow control only, which is a major step in the simplification of controls for future NERVA systems.

Post-test disassembly and examination confirmed analyses that the core structural system had not been damaged by the full-power shutdown transients, and that the restarts had not jeopardized reactor integrity or safety. Analyses of the fuel material pointed up specific areas where additional design work and future development should be emphasized in order to achieve the eventual core lifetime necessary to meet future objectives.

In summary, the reactor system as a whole performed extremely well. In addition, the experimental data agreed with analytical predictions so well that confidence in predicting the behavior of NERVA systems over wide ranges of operating conditions has been increased appreciably.

BLANK PAGE

III. TEST DESCRIPTIONS

The NRX-A3 was tested at the Test Cell "A" (TCA) facility of NRDS. This test cell complex includes the gas storage (hydrogen, nitrogen, and helium), liquid hydrogen (LH_2) storage, piping, and controls systems necessary to complete a test series for the NRX-A size reactor and test assembly. The controls are located approximately two miles from the test cell. Figure 1 is a very simplified sketch showing the key TCA systems used. The frontispiece is a photograph of NRX-A3 located on the test car and connected to TCA.

Figures 2 and 3 show some detail of the reactor mechanical configuration. The reactor system inside the pressure vessel consists of 1626 fueled elements, which make a 132-centimeter long cylinder approximately 44 centimeters in radius containing 172 kg of enriched uranium. About 24.5 percent of the 796,000 cm^3 core volume is coolant channel void (which includes 30,600 axial coolant holes in the fueled graphite), while approximately 14 percent is unfueled graphite. The fueled graphite elements contain 0.417 gm/cc of uranium (enriched to 93.5 w/o U-235) in the central 70 percent of the core and the concentration decreases in six steps to 0.136 gm/cc of enriched uranium at the periphery. Surrounding the core's cylindrical surface is a 5.3 centimeter thick graphite barrel. Next is a beryllium reflector 11.7 centimeters thick containing 12 beryllium control drums of radius 5.2 centimeters, each of which has a boron-aluminum poison vane that moves toward or away from the core center as control drums are rotated. After manufacture, the core reactivity was adjusted with shims to yield a predicted cold critical drum position of approximately 90 degrees (reference 4). The core contained 836 positive reactivity graphite shims and 388 negative reactivity TaC shims. A more detailed description of the reactor can be found in references 5, 6, and 7. Throughout this report specific core locations are referred to by "Station Number" which defines the nominal distance in inches from the dome or cold end for the core.

Prior to testing, the reactor was shipped to NRDS from the assembly facilities of the Westinghouse Astronuclear Laboratory, located a arge, Pa. During shipment the reactor

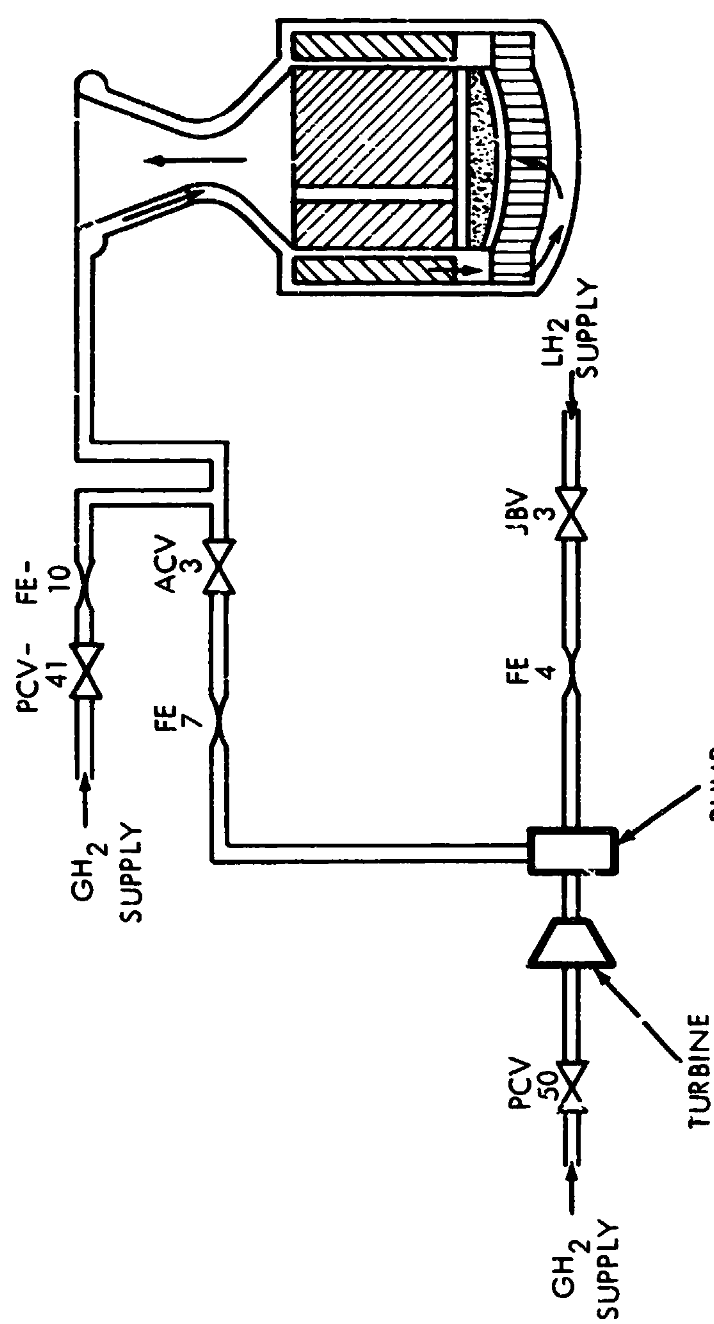

Figure 1. Simplified Test ell "A" Flow Schematic

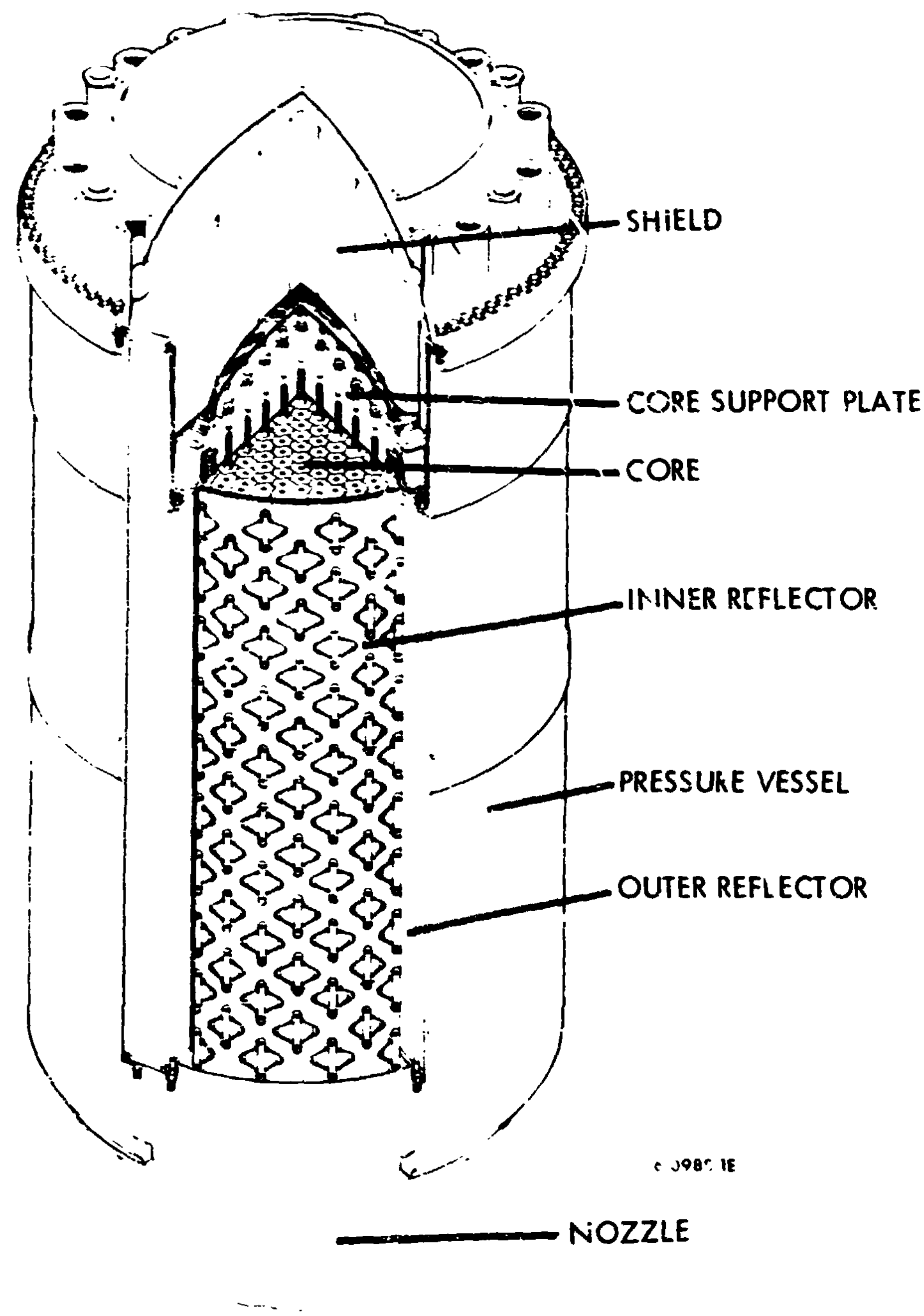

Figure 2. View of NRX-A Reactor

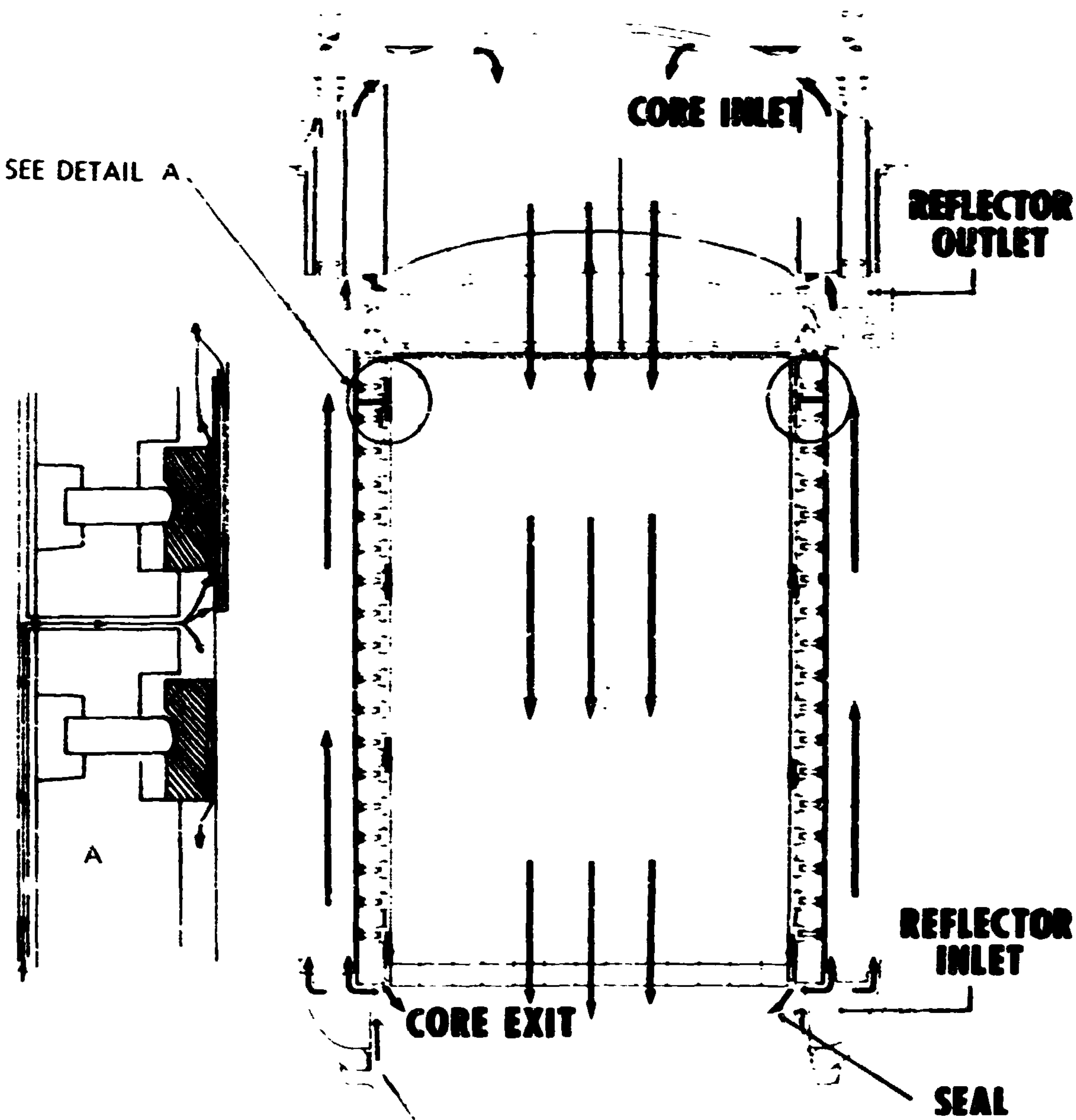

Figure 3. NRX-A Flow Path

contained 6990 B_4C poison wires used to protect against inadvertent criticality. Assembly of the reactor into the pressure vessel, removal of approximately 90 percent of the poison wires, installation of the nozzle, mounting on the test car, and other assembly operations were performed at the Reactor Maintenance, Assembly, and Disassembly Facility (R-MAD) at NRDS. Transfer to TCA from R-MAD on special railroad tracks was performed using a special remote controlled engine. Reference 8 describes in detail the assembly operations.

The basic controls systems used throughout the test series as well as certain new controls concepts which were evaluated are described in Section IV. D.

The NRX-A3 test series was conducted between April 7, 1965, and May 28, 1965, inclusive, and consisted of seven experimental plans (EP's). An experimental plan, in general, defines the tests to be performed during a given time period which is usually one day. The individual tests are designed to carry out the requirements of the NRX-A3 Test Specification (reference 9). Each experimental plan is described below. Detailed results of the tests are described in Section IV.

A. EP-1, INITIAL CRITICALITY AND FLOW TESTS

During this EP, tests were performed to investigate basic nuclear, propellant, and controls characteristics of the reactor system. Specific tests involved were as follows:

1) Initial Criticality was achieved and the remaining poison wires removed. Basic reactivity data and subcritical multiplication data were acquired.

2) The frequency response characteristics of the neutronic power control system were determined and the control drum scram time measured.

3) Tests were performed to check for proper operation of the various key reactor protective devices. These devices include fixed power scram, reactor period scram, floating power scram, period limiter and power limiter.

4) Three ambient gaseous flow tests, two with gaseous hydrogen (GH_2) and one with gaseous nitrogen (GN_2), were performed to determine the reactivity effects of (1) GH_2 and (2) core bundling forces; to check predictions on propellant characteristics of the systems; and to check response of the various pressure transducers.

5) Two liquid hydrogen flow tests were performed to verify revised predictions related to startup profiles, to check response of certain instrumentation channels, and to evaluate the operational techniques with LH_2 pulse cooling planned for use following high power runs.

Throughout the performance of this EP all systems operated satisfactorily. The period and power limiter circuits were being checked out for the first time. Following this checkout, it was decided to use only the power limiter for the remaining tests. The gaseous and liquid flow tests, which were composed of both transient and steady-state operations with the reactor operating at approximately one (1) kw, verified that the flow characteristics of the test assembly were very near the predicted values and indicated satisfactory operations of transducers. The "cold critical" control drum bank position was 89 degrees compared with a predicted 90 degrees.

B. EP-II, POWER CALIBRATION (PHASE I) AND CONTROL DRUM WORTH TESTS

The primary objectives of these tests were (1) to determine the power level calibration of the neutronics channels used in the controls system and (2) to obtain additional control drum reactivity worth data.

During the power calibration phase, uranium - aluminum wires located in the central core region were irradiated while operating the reactor at approximately 10 kw for 20 minutes. Subsequently these wires were radiochemically analyzed for total fission determination and the results, coupled with power distribution data developed during critical experiments at WANEF (reference 10), used to calibrate the neutronics channels.

The differential reactivity worth of one (1) control drum was measured over its entire range from 0 degrees to 180 degrees (full-in to full-out). Integral reactivity worths of individual control drums were measured from the "critical" position to full-out and from the full-in to the full-out position using the positive period technique. The integral worth of each drum was also measured from the full-out to the full-in position using the "rod-drop" technique.

Results of these tests revealed that the reactivity characteristics of the reactor were sufficiently near predictions to permit performance of the planned power tests.

C. EP-III, NEUTRONICS CALIBRATION (PHASE II), LIQUID HYDROGEN FLOW TEST AND SCALED-DOWN POWER TEST

During this experimental plan additional LH_2 flow tests were performed, the flow shutdown protection system (Section IV.D.) was tested, the neutronics system detector positions adjusted, and a scaled-down full power test performed.

Following EP-II the LH_2 turbo-pump was refurbished requiring that its performance be re-evaluated. LH_2 flow tests were performed during EP-III, to provide the necessary data for this re-evaluation, to provide final information on valve sequencing during initial phases of power test start-up, and to provide additional information on the performance of the flow shutdown protection system.

Based on the power calibration data obtained during EP-II the neutronics detector positions were adjusted with the reactor operating at near 100 kw.

A scaled-down full power test was also performed to check out the programmed profiles, systems, procedures, and personnel. This test served as a dry run in which all valves were operated except those which would release high pressure gas or LH_2. The actual full power test power demand profile was used, but with the demand power reduced by a factor of 1000 by the forward positioning of the neutronics sensors.

D. EP-IV, FULL POWER TEST

This test was performed with a start-up ramp designed to effect a $50^{\circ}R$/sec rate of increase in nozzle chamber temperature, with holds at 50 percent and 80 percent power for neutronics system calibration checks, and operation at full power (1120 mw) planned for a duration of time permitted by the facility LH_2 and GH_2 supplies. The power ramp was preceded by an automatic reactor startup (Section IV.D.) to 50 kw. Throughout the power test, time-based demand schedules for LH_2 flow rate, neutronic power, and reactor core temperatures were used.

These controls systems are more fully described in Section IV.D. During startup the LH_2 flow was demanded on a 0.88 lb/sec^2 ramp. A nominal neutronic power calibration correction was made during the 50 percent power hold.

After 203 seconds at full power a spurious spike in the turbo-pump RPM channel caused a flow shutdown and scram followed by automatic introduction of GH_2 from the high pressure gas supply through valve PCV-41. This sytem is designed to provide adequate cooling for the test assembly under such conditions. This control system performed as expected from the controls point of view, however, a characteristic of the piping system, not accounted for by the control circuit, caused insufficient cooling for the reactor tie rods during the gas flow phase. Control of the GH_2 system was switched to manual and GH_2 flow adjusted so that the tie rod temperatures were reduced and held within established limits.

Subsequent data analyses indicated the maximum average tie rod material temperature reached during the transient was approximately 2070°R with a corresponding maximum individual tie rod temperature of 2503°R. A test limit of 1200°R had been established for the average tie rod exit gas temperatures. Tie rod liners reached a maximum temperature of 2800°R.

The probable cause for the RPM overspeed trip which initiated the shutdown was attributed to a loose terminal located in a power supply associated with the RPM circuits.

Reactor and system performance prior to the spurious shutdown was as predicted. Core temperatures and pressures were in agreement with predictions.

E. EP-III-A, FLOW TEST AND SCALED DOWN POWER TEST

Detailed data analyses following EP-IV indicated that the reactor core was capable of a re-start to full power and a GH_2 test was carried out in this EP to determine the pressure drop characteristics of the core for comparison with EP-III data and check out the flow shutdown protection system which had been modified since the EP-IV full power run. These tests indicated that the test assembly was capable of performing an additional full power test.

A second scaled down power test was also performed during this EP in preparation for the following full power test.

F. EP-V RESTART FULL POWER TEST

The startup to full power for this test was performed in the same manner as for the EP-IV full power test. After approximately 16 minutes at power, of which 13.1 min were at full power, the run was terminated upon reaching the limit established for LH_2 usage. A normal shutdown, consisting of a nominal $-50^{\circ}R$/sec ramp was used. Following shutdown LH_2, GH_2, GN_2 and LN_2 were used to complete the cooldown.

G. EP-VI ALTERNATE STARTUP MEDIUM POWER TEST

This experimental plan was performed to investigate operations which differed from those normally used in the performance of full power testing and involved the checkout of certain new control schemes. In general, the tests were performed to:

1) Experimentally map the $1.00 net reactivity feedback line and $1000^{\circ}R$ tie rod temperature line of the steady-state power-flow operating map (figure 4) for nozzle chamber temperatures up to $2500^{\circ}R$.

2) Operate in the medium power range with control drum position fixed and power level changes accomplished by varying only LH_2 propellant flow rate.

3) Check out new controller concepts and obtain dynamic transfer function data.

Since the primary test series objectives were to establish the test assembly characteristics for long durations at full power, this EP was deferred until after the completion of the full power tests. In addition, the maximum allowable temperatures were restricted to a nozzle chamber temperature of $2500^{\circ}R$ in order to minimize further core corrosion which might mask the corrosion effects of the full power runs.

During the mapping test the reactor power and propellant flow rates were varied while experimentally determining points on the $1000^{\circ}R$ tie rod line and the $1.00 net reactivity feedback line. During this test, the newly installed temperature limiter circuit was checked out and found to operate satisfactorily. Figure 4 shows a comparison of predictions with experimental data.

BLANK PAGE

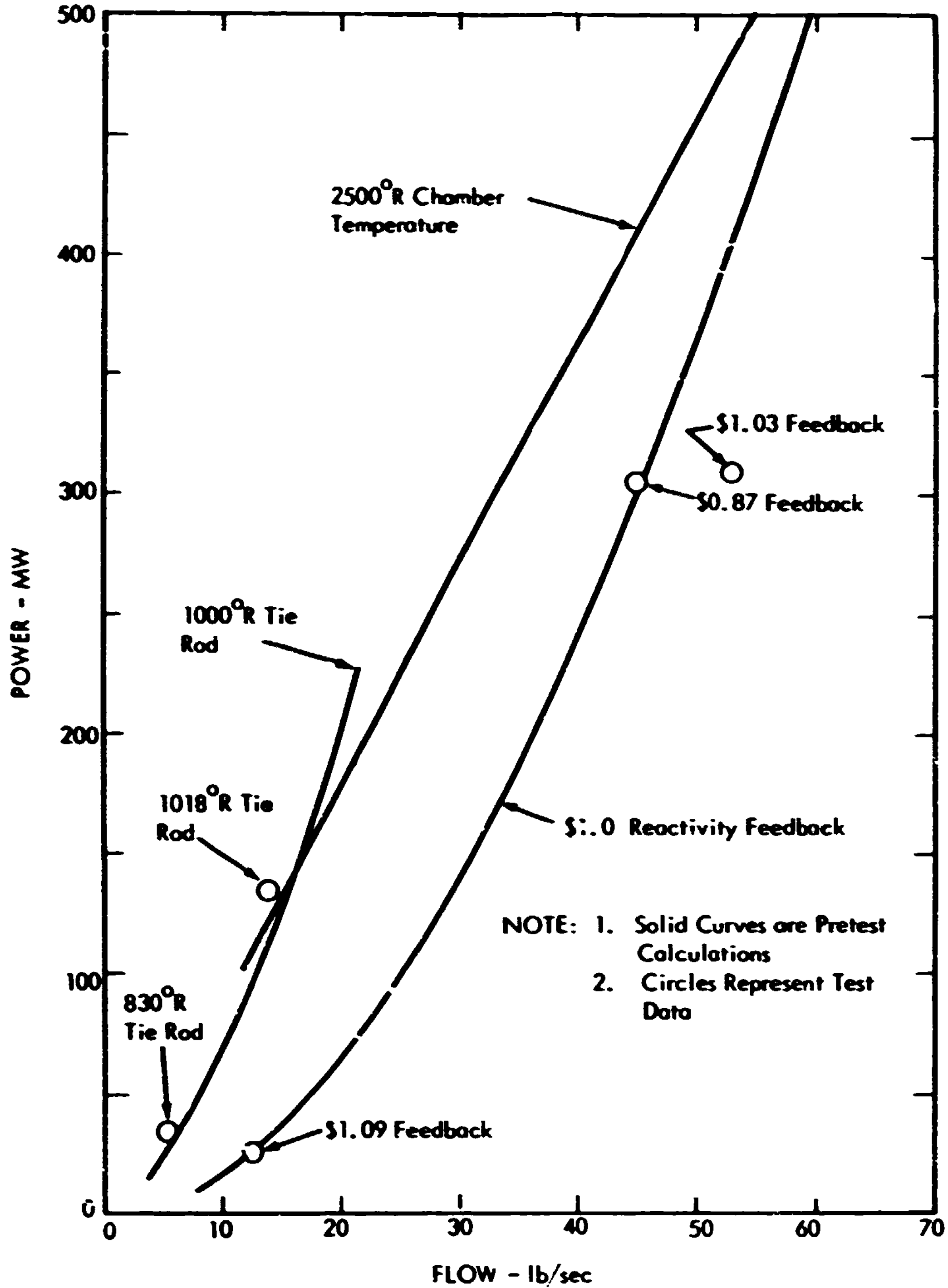

Figure 4. Reactor Operating Map with Experimental Data Points

Of special interest were the experiments performed with control drum position fixed. With the reactor operating at 1 mw and only a purge flow of GH_2, the control drums position was fixed and LH_2 flow rate was manually initiated and increased to 7.5 lb/sec with a corresponding power level increase to about 35 mw.

Later in the EP fixed drum control position was established at about 45 mw and 10 lb/sec LH_2 flow rate. From this point the propellant flow rate was programmed on a 0.88 lb/sec^2 ramp to 45.2 lb/sec which resulted in a smooth power level increase to a nominal 340 mw. The flow rate was reduced to 20 lb/sec on a -0.88 lb/sec^2 ramp resulting in a power level decrease to 95 mw.

Figure 5 shows the LH_2 flow and corresponding reactor power as a function of time. Figure 6 shows the actual path followed on the power-flow operating map. Subsequently a power level adjustment was made and a number of frequency response measurements were performed on various controllers including a new nozzle chamber pressure controller (reference 11).

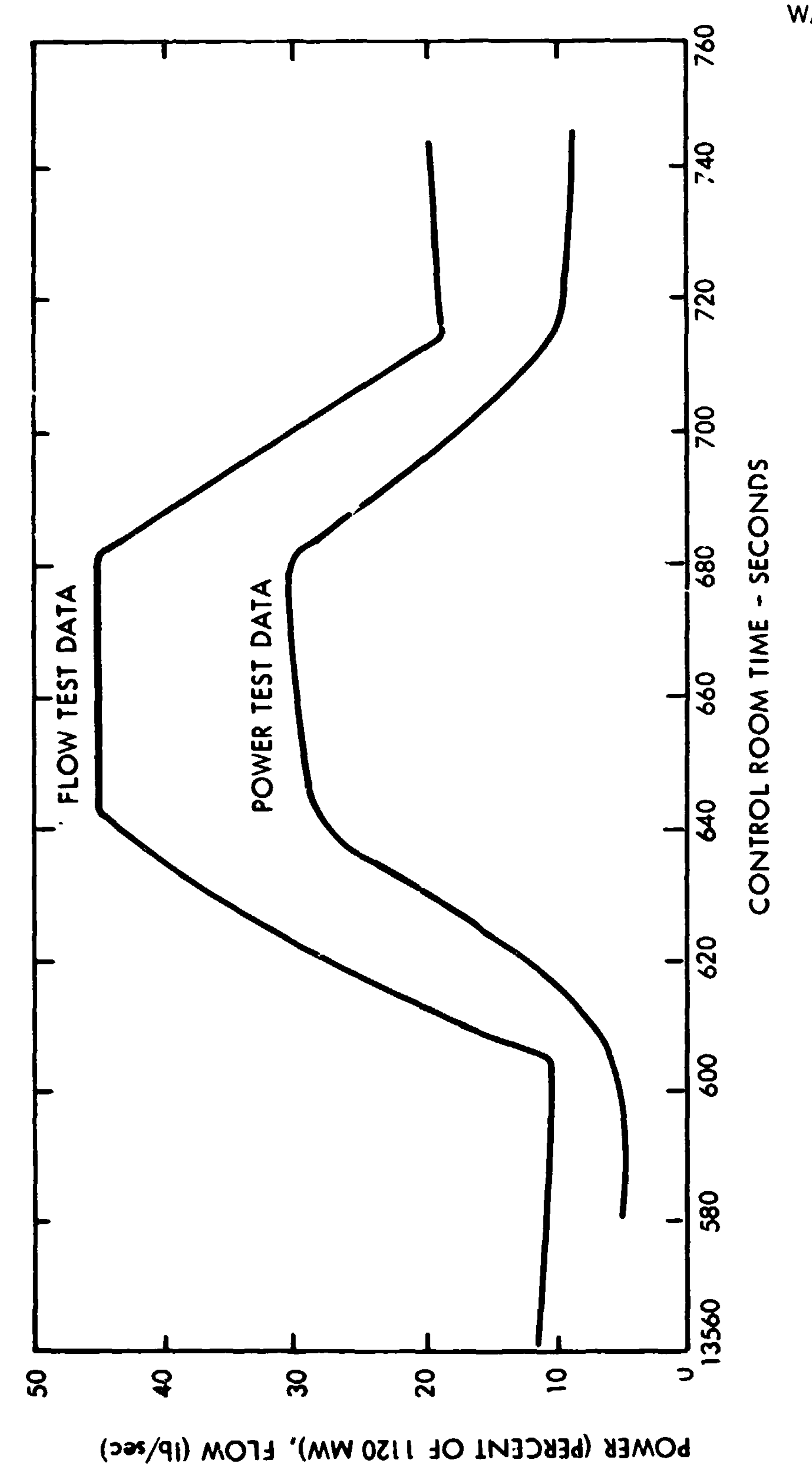

Figure 5. Reactor Power and Flow Vs. Time for Fixed Control Drum Test

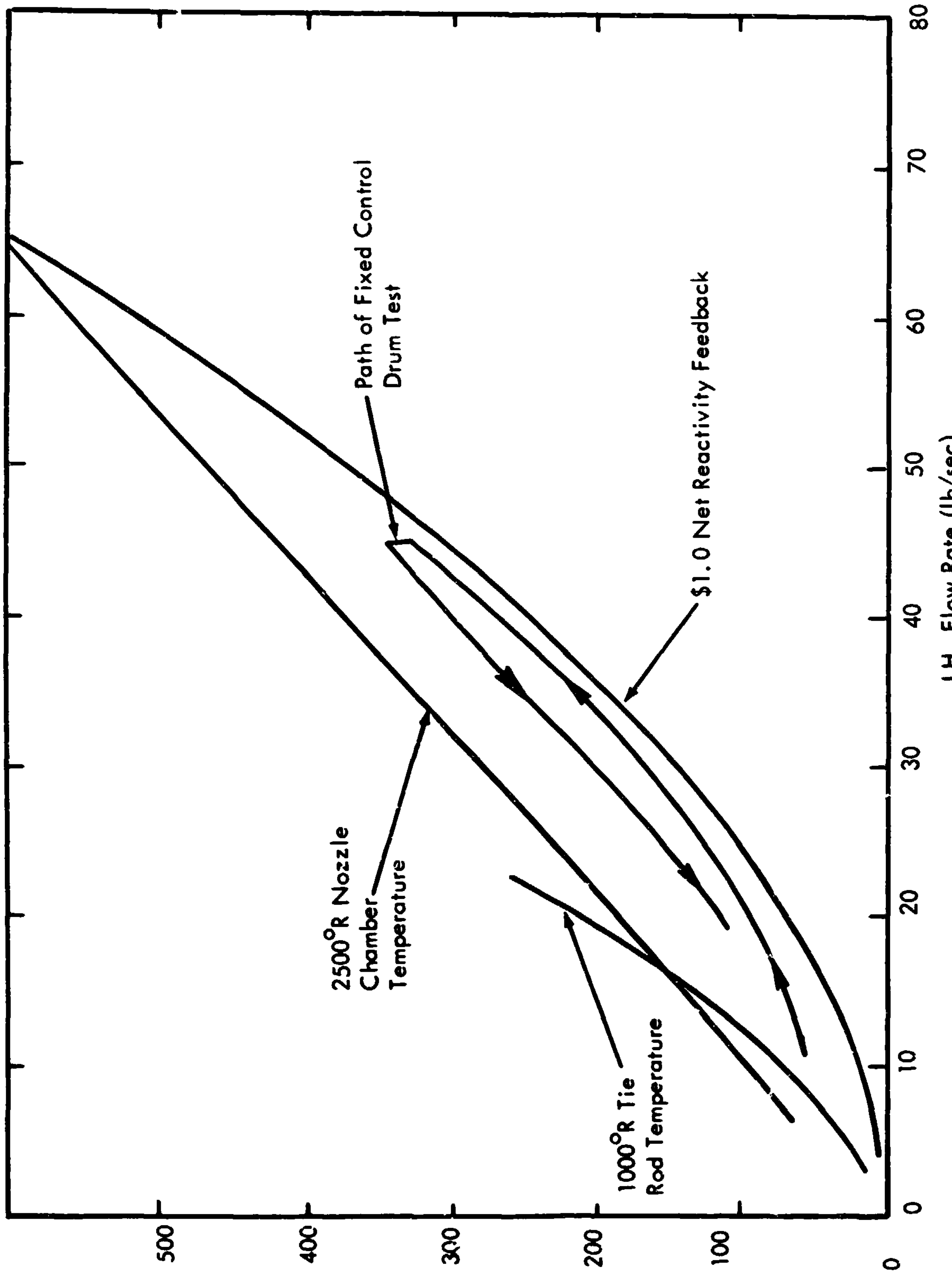

Figure 6. Reactor Operating Map with Operating Path for Fixed Control Drum Test

IV. TEST RESULTS

A. THERMAL AND FLUID FLOW

This section contains a discussion of thermal and fluid flow aspects of the NRX-A3 tests. Generally, good agreement exists between predictions and results for thermal and fluid behavior both at steady-state and transient conditions (reference 12). Predicted values for nozzle, reflector, and core pressures and temperatures, reactivity feedback, and specific impulse as a function of reactor power level for a family of propellant flows, as well as startup and shutdown transients are given in reference 5. Temperature, pressure and hydraulic calculational methods and predictions can be found in references 5 and 6. Reference 13 provides a summary of pretest predictions for each significant test.

1 TRANSIENT BEHAVIOR

In general, good agreement was demonstrated between pretest predictions and test results for the transients associated with startup to and shutdown from full power.

Of interest, however, are (1) control drum bow which occurred during the reflector cooldown transients at the beginning of the ramp to power, (2) inner reflector temperature rise during steady-state operation at full power, and (3) reactor behavior during and following the flow shutdown which terminated EP-IV.

Control drum bowing and torsional rubbing resulted during reflector cooldown in the first power test EP-IV, because of large diametral temperature gradients across the drum, occurring during the transient startup. The control drum bow and the resulting high torques required for movement are functions of reflector and drum initial temperatures and their cooldown rates. This condition did not, however, result in reactor control problems for this test. Additional clearance to prevent rubbing has been incorporated into NRX/EST, and a more symmetric control drum, which would eliminate this problem is designed for incorporation into NRX-A5.

Experience from the NRX-A2 and KIWI-B4E tests indicates that the inner reflector temperature increases during operation, because its thermal conductivity is decreased by fast neutron irradiation. Data from the NRX-A3 test indicated that the thermal conductivity returned to its initial value between EP-IV and EP-V. Additional data and analysis is needed to predict the inner reflector temperature for continuous firings of longer duration.

After approximately 203 seconds at essentially full power during EP-IV, a spurious pump overspeed trip initiated a flow shutdown, which scrammed the reactor and supplied gaseous hydrogen coolant to the reactor through valve PCV-41. The gaseous hydrogen flow rate was insufficient for approximately six seconds causing the core tie rods and tie rod liners to exceed their operating limit. The maximum tie rod and tie rod liner metal temperatures were estimated to be 2503°R and 2800°R respectively based on a measured mean temperature. Subsequent use of analytical models and laboratory tests indicated that a minimum of structural tie rod damage had occurred and that the reactor retained sufficient capability to achieve a restart to full power operation without undue risk. This analysis was confirmed by the subsequent performance of successful power and mapping tests (EP-V and EP-VI). These analytical models, supported by laboratory tests, have proven to be sufficient to define the reactor structural system during severe transients and to provide a valid basis for judgements of reactor conditions following abnormal transients.

Demonstration of a stable power response to propellant flow changes with control drums position fixed was accomplished in EP-V of NRX-A2 and EP-VI of NRX-A3. For a discussion of the NRX-A3 test and graphical illustration of the test results, see Section III.G. of this report.

2 STEADY-STATE BEHAVIOR

During the various flow and power tests of this test series, the system temperatures and pressures were in agreement with pretest predictions. Analysis of pressure data from the gaseous flow tests performed in EP-I indicated agreement between measured and predicted system and reactor pressures. Table 1 shows a comparison of various system parameters with predictions during the three power holds for the first full power test (EP-IV).

Of prime importance in the long range development of NERVA reactor cores is a detailed understanding of temperature distributions throughout the core. Thermocouples located

CONFIDENTIAL

TABLE I

EP-IV STEADY-STATE PARAMETERS

Nominal % Power		50%		80%		100%	
Time (Control Room)		21400		21480		21550	
Computed Power		503 mw		878 mw		1093 mw	
		Predicted	Measured	Predicted	Measured	Predicted	Measured
Nozzle							
Inlet Temp.	°R	45	48	49	50	50	53
Inlet Press.	lb/in^2 abs	481	475	747	730	882	870
Tube ΔP	lb/in^2 differential	63	55	116	105	145	135
Exit Press.	lb/in^2 abs	420	418	631	625	737	735
Flow Rate	lb/sec	50.8	50.8	66.5	66.5	73.5	73.5
Reflector							
Inlet Temp.	°R	94	91	127	120	143	135
Inlet Press.	lb/in^2 abs	418	420	631	625	737	735
Outlet Temp.	°R	155	160	206	220	229	240
Outlet Press.	lb/in^2 abs	397	405	597	605	697	700
Inner ΔP	lb/in^2 differential	94	95	143	138	167	166
Outer ΔP	lb/in^2 differential	21	21	34	33	40	41
Core							
Inlet Temp.	°R	160	167	21[illegible]	216	221	240
Inlet Press.	lb/in^2 abs	390	397	587	587	685	687
Exit Temp.	°R	2693	2565	3315	3503	3905	3898
Exit Press.	lb/in^2 abs	324	325	488	487	570	569
Core ΔP	lb/in^2 differential	66	69	99	101	115	118
Calc. Chan. Temp	°R	2690	2565	3503	3400	3898	3817
Sta. 26 Avg. Temp	°R	2195	2278	3140	3087	3520	3534
Tie Rod Exit Gas Temp. (Avg.)	°R	511	526	587	592	630	644

CONFIDENTIAL

in the unfueled graphite elements are the primary source of temperature determinations during the test series. Thermal capsules located at the hot end of the core, however, provide the best indication of maximum temperatures in the unfueled elements. Consideration must be given, both from temperature control and diagnostic aspects, to the fact that thermocouples located in the unfueled modules throughout the core indicate a considerably higher temperature than temperature of the fuel itself for two reasons: (1) high radiation heating in the sensor and in the unfueled module containing the sensor and (2) gaps between the sensor and the unfueled module, and between the unfueled module and the fuel elements. In NRX-A3, the thermal capsule and thermocouple data exhibit good agreement. The calculated value of maximum fuel temperature at core centerline agreed within 35°R of the 4600°R obtained from regression analysis of measured data.

Deviations from the anticipated radial temperature distribution were observed and were attributed to the inlet temperature being lower than expected (225°R vs. 250°R) and to the control drum bank operating at an angle other than that for which the core had been orificed.

Station 20 thermocouples indicated an increasing temperature with time at full power. This is attributed to interstitial mid-band corrosion, which increased the gap between the central unfueled element that contains the thermocouples and the fueled element. The slowly increasing gap reduced the heat transfer away from the thermocouple, causing its temperature to rise with time at a constant power level.

The tie rod exit gas temperatures, calculated after the tests from available data, were lower than values measured during operation. The variation between calculated and test values are attributed primarily to the use of lower values of thermal conductivity of the insulating sleeves than actually exist in the test environment. Testing is in progress to confirm this point.

The EP-VI mapping test indicated that large asymmetries in hydrogen flow and material temperature distributions exist at flow rates below 13 lb/sec. This effect was also observed on NRX-A2 at flows below 10 lb/sec. The cause is attributed to two-phase flow at the reflector inlet plenum, where temperatures and pressures are substantially below the critical point of 60°R and 180 psia. This asymmetry condition also causes unusually large deviations between predicted and measured reactivity feedback (reference 12).

E. MECHANICAL EVALUATION

Information for the evaluation of the mechanical performance of NRX-A3 originates from two sources: (1) data obtained during the tests from dynamic instrumentation and (2) data from post-operative examination during and subsequent to reactor disassembly. In the section which follows, the instrumentation utilized and the pertinent parameters which were measured are described. The observations and analyses made as a result of post-operative examination are outlined in Section IV.F., Disassembly and Post-Operational Examinations.

Analysis of transducer data and post-operative evaluation of all reactor components, following disassembly, showed that the reactor performed extremely well structurally, and was generally in excellent condition following the tests.

Results of data analysis showed that the radial and axial core expansions agreed well with calculations. Evaluation of tie rod strength after the high temperature excursion of EP-IV indicated that the core axial support system was structurally sound. Measured tie rod loc agreed well with calculated values and the core generally remained concentric throughout the test series.

In addition there was no indication of excessively large motions or any serious threats of self-excited vibrations.

The flow tests and power tests were performed without serious damage to the reactor in general, although there was some component damage, as discussed in Section IV.F.

1 DATA ANALYSIS

The instrumentation utilized to obtain dynamic information during the tests included strain gages on the fuel element tie rods and lateral support leaf springs, displacement gauges between the inner and outer reflector, external accelerometers on the pressure vessel and nozzle, and torque transducers on the control drum drive shafts. Observations made with this instrumentation are as follows:

a) Lateral Support Spring Performance

Twelve lateral support leaf springs were instrumented with weldable strain gauges to monitor core radial motion. The instrumentation was designed to detect only relative displacement between the core and inner reflector assembly. Circumferentially variable core expansion would be revealed as asymmetric gap changes between the core and inner reflector. Rotational motion of the core would not be detected.

It had been predicted prior to the NRX-A2 test that some plunger pins might stick in the inner reflector. Evidence appeared in the NRX-A2 data which indicated that one of the plunger pins did stick for a short time during the shutdown from the high power run (reference 14). To eliminate this problem in NRX-A3, the plunger pins were select-fitted for the mating holes to insure proper clearance. Review of NRX-A3 data revealed some chattering on a few of the data channels, indicating some evidence of very slight sticking, but the duration and magnitude were very small in all cases. It is concluded that the selective assembly has eliminated any serious sticking in the lateral support system.

The core inner reflector gap was measured during ambient gas flow conditions, with no appreciable thermal effects present, during EP-I. This data was used as a check on predictions. The data from EP-III-A was later used as a further check on the EP-I data. Prior to the power tests, EP-IV and EP-V, calculations were made to determine the predicted change in radial gap at the aft end of the core, where clearances are at a minimum during operation. Calculations predicted no interference, and the data obtained during the runs show none. In addition, all available data indicated that the core remained essentially concentric during operations, and there was no indication of contact between the core and the inner reflector. Test data also indicated essentially no significant vibrations of the support springs.

For detailed explanations of calculational methods utilized, data analysis, and any minor discrepancies noted, references 15, 16, 17, 18 and 19 will provide more complete information.

b) Tie Rod Performance

Six of the 289 tie rods which provide axial support of the core were instrumented with two weldable strain gauges. The tie rods are essentially loaded in axial tension, although some bending can occur when the core is bundled.

The measured loads on the tie rods were consistent between the two power runs, EP-IV and EP-V, and in all cases were less than the computed values.

During the shutdown operations of EP-IV, the maximum average exit gas temperatures at the aft end of the tie rods exceeded the 1200°R limit (reference 18). Some of the central rods experienced material temperatures in excess of the 1760°R aging temperature, even as high as 2503°R. In order to arrive at a decision to attempt a full-power restart (EP-V), it was necessary to determine if the tie rods were critically damaged as a result of the overheating, and if they were capable of sustaining full power loads in the weakened condition.

Extensive analysis of the data and further tests on tie rods showed that sufficient strength remained in the tie rods to sustain the loads to be encountered in a restart to full power. In addition, it was calculated that the bundling forces present in the core had prevented gross slipping in parts of the core, thereby preventing any appreciable local yielding in the tie rods. The result of the analyses was a decision to perform EP-V as planned, after an interim test (EP-IIIA) designed specifically to check for obvious damage. Subsequent post-operative inspection of the tie rods revealed no visible damage (Section IV.F). In summary, the tie rods system survived the high temperature excursion of the EP-IV shutdown and performed during EP-V without fault.

c) Accelerometer Results

Results from the accelerometer measurements indicate that accelerations up to 3 g were observed on the pressure vessel. These acceleration levels occurred at reduced power levels (or reduced flow levels for ambient tests), and became appreciably reduced when full power conditions were reached. These occurred at relatively high frequencies of 240 and 350 cps and over band frequencies of 80-120 cps and 480-560 cps.

Acceleration levels of 30 g were reported on the nozzle during EP-IV and EP-V. A nozzle resonance of 240 cps has been well defined from NRX-A2 shake tests (reference 20) and has been confirmed by Aerojet-General Corporation from past laboratory tests. The source of excitation is believed to be the oscillation from separated to full flow in the nozzle at reduced chamber pressure levels.

d) Control Drum Torques - Drum Rubbing

Because of the temperature distributions within the components, both the control drums and the outer reflector sectors tend to bend or bow during the initial cooldown immediately after flow initiation and prior to reaching substantial power levels. The control drum bow tends to be relatively larger than that of the sector, since the side of the beryllium cylinder adjacent to the control vane is exposed directly to the fluid and cools more rapidly than the opposite surface. Since each sector is cooled somewhat symmetrically, its distortion is smaller than that of the drums.

In six of the seven startups, rubbing was slight or non-existent. In EP-IV more severe rubbing occurred in every drum. The rubbing manifested itself in abnormally high drum actuator torque values. Reversal of the high torque values when drum rotation was reversed indicated that a frictional (or rubbing) type of resistance did exist. In subsequent tests prechilling was employed and the rubbing was avoided. To avoid the necessity of prechilling for NRX/EST, the clearances between drums and sectors have been increased by an additional 0.023 inches.

C. NUCLEAR ANALYSIS

1 NUCLEAR

Initial criticality was achieved during EP-1 with 378 poison wires remaining in the core and the control drums at 168 degrees (delayed critical). This compared very well with pretest predictions (reference 12). Pretest predictions were derived in part from critical experiments performed at WANEF prior to the NRX-A3 testing (reference 10)

The measured cold critical control drum bank position with no poison wires was 89 degrees, 1 degree less than that attempted by shimming the core before the tests. Details are given in references 12 and 4. Inverse multiplication during poison wire removal and during the approach to criticality is given in references 21 and 8 for the test results and in reference 13 for the predictions. The neutron economy is given in reference 5.

The control drum bank reactivity worth was determined to be 8.8 $\pm$ 0.3 dollars. The total control drum bank swing required to perform the test series was 2.4 dollars plus 2 dollars for the safety margin limit, or 4.4 dollars. This compares with 4 dollars for the NRX-A2 series (reference 12). Differential bank and individual drum worth measurements are found in reference 21. Predicted differential and integral drum bank worths are in references 5 and 13.

Reactivity measurements were in good agreement with predictions in references 5 and 13. Core weight loss, from corrosion and erosion, determined from cold criticality measurements before and after the power tests, was in good agreement with measured weight loss. This and other reactivity changes are discussed in reference 12. A reactivity computer, an on-line electronic instrument for continuous recording of reactivity, was used and is discussed in reference 21. Calculated reactivity change from cold to hot conditions was within 10 cents of the measured data obtained at zero and full power. The cold to hot reactivity formula (i.e. hydrogen and temperature reactivity coefficients), reflector material reactivity coefficients, the in-hour equation relating excess reactivity to reactor period, iso-reactivity plots of reactor power versus H_2 flow rate, and nuclear computer codes can be found in reference 5. Core reactivity coefficients for carbon, niobium, stainless steel, and Inconel-X, and reactivity versus poison wire inventory can be found in reference 5.

The radial power distribution determined from gross ionization measurements on each fuel element was within nine percent of the calculated distribution. Fissions per gram measured at the core periphery differed only 4.7 percent from calculations. Details are in reference 12 for both measured and predicted power distributions, in reference 5 for predicted radial and axial power distributions, and in reference 22 for measured radial and axial distributions.

2 REACTOR SAFETY

Reactor safety was provided by limitations in reactivity change magnitudes and rates. Various possible accidents were analyzed to determine the extent of personnel hazard.

A minimum reactivity shutdown capability limit of 2 dollars was established for the control system. The reactor period scram was set at 0.3 seconds for operations at less than 100 mw. Maximum control drum withdrawal rate was limited to 55°/second, while the scram velocity was limited to a minimum of 240°/second. Throughout the test series constant attention was given to these nuclear safety parameters and test results indicate no nuclear safety problems.

An accident analysis giving excursion magnitudes and other consequences of various accidents can be found in references 23 and 24. A fission product release analysis giving radiological consequences is given in reference 23.

3 RADIATION

Calculated heating rates in calorimeter materials external to the reactor were generally lower than measurement by 2 to 100 percent depending on location. Analytical methods and computer codes are found in reference 12. Good agreement in experimental data between NRX-A2 and NRX-A3 was observed. The calculated heating of reactor components is generally lower than measured by six to thirty percent (reference 12). Analytical methods of determining reactor component and calorimeter heating are found in references 12 and 25.

Neutron and gamma spatial distributions outside the reactor and gamma dose and fast neutron flux inside the reactor were measured by dosimetry. The predicted fast neutron flux is, in general, underestimated both internal and external to the pressure vessel. Large scatter exists in the data and improvement in measurement techniques and the normalizations is warranted. The calculated internal gamma dose rate measurements at the core midplane compare within ± 10 percent of measurements. The external gamma dose rates measured on the reactor midplane about 5 feet from the core centerline showed considerable scatter leaving the uncertainty in calculations at ± 30 percent. Analysis of the gamma dose rate under the privy roof indicates that the test car secondary gamma radiation is the predominant source. More detail about gamma dosimetry using thermoluminescent detectors and fast and thermal neutron dosimetry using copper, cobalt, gold, and nickel can be found in reference 26. Reference 21 provides additional information.

Calculated values exist of fast neutron energy spectra inside and outside of the reactor and thermal neutron spectra inside the reactor. Values and analytical methods for fast neutron flux spectra outside the reactor are in reference 27, which are supported by measurements. An evaluation of methods for calculating spectra inside the reactor is found in reference 25; while values of fast and thermal neutron spectra inside the reactor are found in reference 5.

Gamma source strength (mev/sec) as a function of time after irradiation is given in reference 28 for fission products and activated components from the core, reflectors, and aluminum shield. Beta and gamma decay power after full-power runs is given in reference 5.

D. INSTRUMENTATION AND CONTROL PERFORMANCE

1 CONTROL SYSTEMS

During the NRX-A3 tests, the normal control system consisted of two basic loops: the LH_2 flow control loop, and the reactor power and temperature control loop. Control loops were also provided to furnish controlled reactor cooling during shutdown phases of operation.

In addition, several new control concepts were verified during the NRX-A3 tests. These new control concepts include limiter circuits, pressure control system, and coupled pressure-temperature control system.

Oscillation tests were conducted to obtain transfer function information on the control system, feed system, and reactor during power range operation.

a) Systems Description

The NRX-A3 control systems consisted of the normal NRX control systems used during the NRX-A2 tests and new controllers installed to increase the system r ability and to gain experimental verification of control concepts to be used in the engine control system.

1) Normal NRX Control System

The normal NRX control systems consisting of an LH_2 flow control loop and a temperature and power control loop are described in detail in references 29, 30, 31, and 32. In addition to these basic control loops, there are control loops which provide cooling during shutdown phases of reactor operation.

The LH_2 flow control system consists of a pump specific speed control loop and an RPM/flow control loop. The specific speed loop insures compatibility between the turbopump and the reactor characteristics. This is accomplished by bypassing, if necessary, sufficient flow to maintain a preset pump specific speed. The RPM/flow loop provides a position signal to PCV-50 which controls the gas driving the pump turbine. Valve position in this loop can be controlled by either manual control, pump RPM control, or LH_2 flow rate control.

The power and temperature control system provides a position signal to the reactor control drums. This system provides for manual drum position control, reactor power control, reactor temperature control, and automatic startup of the reactor. In manual drum control, the control drum position demand is provided directly, whereas in manual or programmed power control, the control drum position is generated from a compensated error between measured and demanded neutronic power. The neutronic power feedback signal is supplied from ion chambers located in a water tank positioned in the test cell wall adjacent to the reactor. In temperature control, power demand is trimmed by a compensated error between the measured and demanded temperature. This trim is the incremental power demand which is required to zero the temperature error. The measured temperature used by the controller may be exit gas temperature, Station 26 core temperature, or Station 32 core temperature. Automatic reactor startup is used to bring the reactor from a sub-critical shutdown condition to a preselected power level by programming the control drum position until the selected power level is reached (reference 33).

Following an LH_2 flow shutdown, the reactor is cooled by GH_2. The PCV-41 pressure control system provides a position demand to valve PCV-41 (figure 1) in order to maintain the pressure upstream of FE-10 at a level such that the nozzle torus pressure is 60 percent of the pressure level that existed at the time of flow shutdown (reference 34).

In the event of damage to the propellant feed system, emergency cooling would be provided (manual initiation) to the reactor by flowing GH_2 through the reactor dome. This flow would be controlled by valve PCV-18. The PCV-18 position demand is generated from the GH_2 upstream pressure to give a predetermined flow rate.

2) New Control Systems

Control concepts installed for the first time during the NRX-A3 tests include limiter circuits, chamber pressure controller, and slaving of pressure and temperature. References 35 and 11 provide a detailed description of these controls concepts.

The limiter circuits monitor critical reactor parameters: reactor power, reactor period, core temperature, and tie rod temperature. If any of these parameters exceed a predetermined level and if the limiter for that parameter is active, a signal is supplied to the power controller which commands an inward movement of the control drums sufficient to constrain the system variable within its maximum allowable limit.

The chamber pressure control system provides a trim on the flow demand of the LH_2 flow control system. This trim is the incremental flow demand which is required to zero the pressure error. The trim is generated from a compensated error between measured and demanded pressure.

The temperature control system and the pressure control system are inherently coupled in the nuclear subsystem. These systems were coupled externally during one phase of EP-VI by deriving the temperature demand from the measured chamber pressure. The relationship between the measured chamber pressure and the demanded temperature was selected to maintain a tie rod temperature of 800°R.

b) Testing and Results

The NRX control systems were used throughout the NRX-A3 test series. In addition, the new control concepts were checked out and oscillation tests were conducted to obtain transfer function measurements.

1) Normal NRX Control Systems

The LH_2 flow control loop and the temperature and power control loop were used during the NRX-A3 tests with no abnormalities occurring. These control loops performed as predicted. Agreement between the planned and measured parameters was within the accuracy of the data system (reference 36)

The automatic startup system was used to bring the reactor to power on essentially all startups, and functioned as predicted. This system had been redesigned between the NRX-A2 and NRX-A3 tests to eliminate some operational problems experienced during the NRX-A2 tests (reference 31).

2) PCV-41 Pressure Controller

The spurious turbopump overspeed trip which occurred during EP-IV caused a flow shutdown. Upon initiation of the flow shutdown, the PCV-41 pressure control loop was activated to maintain the pressure at P-041 (upstream of flow venturi FE-10) at a level designed to maintain the nozzle torus pressure at 60 percent of its value just prior to flow shutdown. The pressure controller did provide the P-041 pressure at the desired value. However, after the residual LH_2 was expended from the feedsystem, the gas flow increased and venturi FE-10 became choked; consequently the nozzle torus pressure dropped below the desired 60 percent value even though the pressure control loop error was zero. Because of this condition, the nozzle torus pressure was not maintained at the desired value and insufficient flow was delivered to the reactor.

The PCV-41 valve control was switched to the manual control mode within a few seconds after the shutdown. When the control mode was switched, a sharp further reduction in ambient GH_2 flow occurred. An investigation revealed that this problem was caused by the PCV-41 followup circuit being wired improperly. The combined effect of the choked venturi and the switch in control modes reduced the ambient GH_2 flow considerably below the desired value and resulted in overheating the reactor tie rods.

In order to prevent a recurrence of this flow shutdown discrepancy during subsequent testing, the PCV-41 pressure controller was redesigned to compensate for choking in the venturi, FE-10. The redesign of PCV-41 pressure controller consisted of modifying the P-041 pressure demand to compensate for the pressure drop across the venturi. The modified P-041 pressure demand was 60 percent of the nozzle torus pressure at the time of flow shutdown, with an increase to 120 percent after two seconds. This change in P-041 demand was necessary to account for initial subsonic flow through the venturi increasing to sonic flow after the LH_2 has been expended from the system.

The PCV-41 pressure control system was modified and checked out during EP-IIIA. The controller performed satisfactorily during these checkouts. References 37, 38, 39, 40 and 41 provide information on the PCV-41 system.

3) Limiter Circuits

The power and period limiters were checked during EP-I. For this test the power limiter setpoint was set to maintain power below 0.4 kw. When the power was demanded to exceed this setpoint, the power limiter functioned properly and prevented the power level from exceeding the 0.4 kw.

The period limiter was checked at limiter settings of 10, 5, and 2 seconds, and corresponding period demands of 8, 3, and 1 seconds, respectively. At a setting of 10 seconds, the period limiter worked satisfactorily. At settings of 5 and 2 seconds, slight power oscillations were observed when limiting occurred. Such power oscillations were expected with fast periods.

The power and period limiters were also checked while operating simultaneously. Both power and period were limited to their respective setpoints without significant power oscillations. Following checkout, the power limiter was used for all subsequent runs, and the period limiter was deactivated.

The core temperature limiter and power limiter were checked during EP-VI. With the reactor operating at steady-state, the temperature limiter was checked by reducing the temperature limiter setpoint below the demanded temperature. The core temperature was reduced as predicted. With the temperature limiter still active, the power limiter setpoint was reduced below the demanded power to check the interdependence of the two limiters. Both power and temperature were reduced as expected.

4) Chamber Pressure Control and Coupled Pressure Temperature Control System

The chamber pressure control system and coupled pressure temperature control system were used for the first time during EP-VI. Since the NRX-A3 was the first reactor to contain a pressure control loop and a slaved pressure temperature control system, the test was designed to show that the pressure loop was stable and that the loop performance was as predicted from analog computer and mathematical analyses.

The test results indicated that the chamber pressure control system and the coupled pressure-temperature control systems were stable with larger margins than had been predicted. Because of feed system attenuations and phase lag not accounted for in the analog model, the system band width of the pressure loop was less than predicted.

Operational characteristics of these control systems have not been established, and a redesign of the pressure controller can be undertaken to improve the response time of the pressure control system.

2 INSTRUMENTATION

a) NRX-A3 Transducers

There were a total f 292 WANL sensors installed for the NRX-A3 test series, of which 93.8 percent were operating at the conclusion of the tests. After complete assembly of the test article at NRDS, 98.6 percent of the instrumentation was operable. The operable percentage during EP-I, EP-II, and EP-III was 98.0 percent, and during EP-IV, EP-V, and EP-VI, 93.8 percent were operable.

The major sensor development consisted of high temperature in-core thermocouples. The thermocouples installed at station 32 in NRX-A3 were expected to deviate from the Hoskins calibration at about 3500^{o}R. A special calibration, deviating from the 1962 Hoskins calibration for the tungsten/tungsten-26 rhenium thermoelements, was used to compensate for the expected error. A permanent improvement in the insulation resulted from "conditioning" during the EP-IV run as evidenced later in the EP-V test. The output signal level closely approximated the original Hoskins calibration for the thermocouples. The degraded performance characteristic of a thermocouple with insulation shunting was clearly missing. The fact that "conditioning" had occurred was borne out later in laboratory experiments (reference 42).

Strain gage accelerometers were installed on the pressure vessel for evaluation alongside the piezoelectric type. These accelerometers operated throughout EP-I and EP-VI and the data appear to be correct. LVDT's were also installed for evaluation and data obtained correlated very well with analytical calculations and with pressure and temperature measurements. Further tests of these transducers are needed to fully qualify them for reactor use.

In general, all transducers functioned as well as expected. The anomalies which occurred during test are reported and evaluated in references 43 and 21.

During disassembly no sensor condition was observed which had not previously been determined. Post-operative examination revealed no visual degradation of transducers due to normal test environment. However, the tie rod thermocouples were damaged when exposed to temperatures beyond their design limits during the EP-IV shutdown. Disassembly and post-operative examination results are further reported in reference 43.

b) NRX-A3 Data System Performance

Data system performance is defined as the performance of the instrumentation, data acquisition and data reduction systems at NRDS and WANL. A description of the NRX-A3 data acquisition and reduction systems and their operation can be found in reference 44.

1) End-to-End Checkout

A more extensive end-to-end instrumentation checkout was conducted on NRX-A3 than on previous reactors. The purpose of the checkout was to (1) verify and document the continuity of each channel from the closest termination point to the transducer on the test assembly to the recording device at the Control Point, (2) verify and document the polarity of each channel, and (3) verify and document the gain or setup range of each channel. For those accessible channels, the transducers were stimulated over the range of the instruments. The results show that the recorded outputs of these channels agreed within approximately 0.1 percent of the values recorded during the calibrations of the transducers. Those channels that were inaccessible were checked out to the Control Point by injecting simulated signals at the closest termination points to the transducer located on the Test Assembly.

2) Data Evaluation Team

During this same period of time a data evaluation team was established for the purpose of evaluating the performance of the data system. Following a review of the documents used in establishing the system, an evaluation of all data from EP-I was conducted. The team was composed of members from AGC, EG&G, NTO, and WANL, although for subsequent experimental plans only EG&G and NTO participated. The introduction of this evaluation team concept proved effective and will be continued for future test series.

3) Performance Summary

Before the start of EP-IV, the data acquisition system contained 869 channels of which 508 were in the reactor diagnostic system. During EP-IV, 839 data channels (96.5 percent) operated properly; however, partial data was produced by 10 of the 19 data channels canceled due to discrepancies during this test.

Before the start of EP-V, the data acquisition system contained 850 channels (97.8 percent). During EP-V, 824 data channels (94.8 percent) operated properly; however, partial data were produced by 20 of the 26 data channels canceled due to discrepancies during this test.

Prior to the start of EP-VI, the data system contained 798 channels (91.8 percent). During EP-VI, 770 data channels (89.6 percent) operated properly. Had there been another experimental plan to perform, only 4 (0.44 percent) of the 19 channels displaying discrepancies during this test would have been canceled. Thus, the data system contained 794 working channels (91.4 percent) at the end of EP-VI.

Multiplexer problems were encountered during EP-IV, EP-IIIA, EP-V, and EP-VI. An evaluation of the components involved did not establish the cause of the anomalies. Test evaluations after each experimental plan did not uncover any discrepancies; however, it is suspected that radiation levels became high enough to cause the problems. The total integrated dose measured in the ELR of Test Cell "A" from EP-V was greater than 450 REP near the instrument racks.

The performance of the data acquisition system during the NRX-A3 test series was, in general, good. Following each experimental plan, all the data was reviewed by NTO and an evaluation made with respect to performance. Discrepancies of transducers, data acquisition system, or data reduction system are noted in references 45, 36, 37, 38, 41, 46, and 21.

E. SYSTEMS TRANSIENT BEHAVIOR ANALYSIS

Efforts in the analyses of systems transient behavior were performed in four categories, as described below:

1 PRE-TEST PREDICTIONS

Each planned test in the power range was simulated before the test on the digital and analog computers to predict the performance of the test system. Evaluation of various programmed profile demands led to the choice of demand schedules used later in the reactor test series. The planned tests were demonstrated as compatible with the NRX-A3 control systems on the analog computer by initiating holds at any stage of the profile without introducing dynamics problems.

The computer was used to establish limitations on the allowable rate and extent of the programmed shutdown. Computer results were used to demonstrate the dynamic stability of the fixed drum test and established acceptability of this control mode for use in the NRX tests.

The tests involving transfer function measurements by the sinusoidal and pseudo-random input signal techniques were also simulated. The results were used to determine input signal amplitudes and bandwidths in order to yield meaningful data and to remain within safe operating tolerances. It was demonstrated that a useful signal input for the transfer function tests could be of smaller amplitude with the pseudo-random technique than with the sinusoidal technique.

2 PRE-TEST MALFUNCTION ANALYSIS

Much of the dynamics analysis effort was devoted to predicting system performance during emergency operation, using the analog computer. One class of abnormal or emergency operation involved running the programmer drums in all possible modes of operation, i.e., forward or reverse at 2-1/2 times the normal rate. The modes of abnormal operation involved are retreat, fast retreat, and fast forward. The results indicated clearly that the control systems and reactor system performed well in each of these modes as long as the retreat or fast forward was not continued below a propellant flow rate of approximately 12 lb/sec (in which region high tie rod temperatures might result). The procedures therefore were written to produce a scram or flow shutdown before approaching this low-flow low-power region.

A second class of abnormal operation or malfunction involved the limiters. Checkout of the limiters was undertaken from two approaches:

a) Actuation of limiters from failure of control components or severe system transients.

b) False actuation of limiters resulting from failure of components within the limiters.

Analog computer predictions indicated that the limiters provided ample time for system compensation by the operator in cases of severe system transients and failure of control components. Single failures within the limiters themselves produced no transients in the overall control system.

3 CROSS-CORRELATION AND SINUSOIDAL TRANSFER FUNCTION MEASUREMENTS

Cross-correlation and sinusoidal transfer function measurements were performed successfully during the NRX-A3 test series. From these dynamic measurements, results were obtained which are useful in improving both dynamic models of the system and the control systems for use in future tests. References 47 and 48 provide details.

During facility flow tests prior to receipt of the test article at TCA, an orifice plate was used at the exit of the propellant feedline to simulate reactor impedance. In the cross-correlation measurements, a pseudo-random signal applied to the pump RPM demand was used to perturb the feed system while at 40 lb/sec flow. Using cross-correlation techniques, transfer functions relating the turbine control valve position, pump RPM, flow, pump exit pressure, and feedline exit pressure were computed at frequencies up to 20 cps. The results showed good agreement with sinusoidal measurements made during the same test, confirming the accuracy of the technique. Moreover, results of high precision were obtained at substantially higher frequencies than were possible with the sinusoidal technique.

In the EP-IV full power test, a pseudo-random turbopump RPM demand signal (with a useful bandwidth of about 6 cps) was inserted into the flow control system. Measurements of pressure responses at various locations from the nozzle torus to the core exit permitted the determination of the transfer functions relating these variables up to a frequency of about 6 cps. Comparisons of these results with frequency responses obtained from analog computer models showed generally good agreement in the dynamic behavior of the overall test article, with minor, generally compensating, discrepancies for the individual components. The detailed results of these transfer function measurements using cross-correlation techniques have been reported in reference 48.

Five frequency response tests were planned for EP-VI:

a) In control drum position control and pump RPM control, oscillate RPM demand preceded by a step in RPM demand.

b) In control drum position control and pressure control, oscillate pressure demand preceded by a step in pressure demand.

c) In power control and LH_2 flow control, oscillate power demand preceded by a negative step in power demand.

d) With temperature demand slaved to measured pressure, oscillate pressure demand preceded by a step in pressure demand.

e) In control drum position control and LH_2 flow control, oscillate drum position demand preceded by a negative step in drum position demand.

The purpose of these control tests was to obtain transfer function information on the control system, feed-system, and reactor during power range operation.

Test a) was not performed because PCV-50 was very near its closed position, and it was felt the oscillation magnitudes necessary to acquire data might cause valve damage by hitting the valve seat.

Tests b) and d) were intended to evaluate the chamber pressure control loop and coupled pressure-temperature system as described in Section IV.D. The results indicate that these systems operate in a stable manner and have somewhat wider stability margins than predicted. This data will be used to optimize the new control concepts. The test data verified feedline, nozzle, reflector, and core analog models to approximately one cps. However, the data showed an amplitude attenuation in the turbopump which was not predicted by the analog computer model.

Test c) yielded the desired data on the reactor flux loop and showed minor discrepancies between the test results and the analog computer model at high frequencies (above four cps).

Reactor power data from test e) was reduced and the transfer function of reactor power versus control drum angle was obtained. The temperature data which was desired from this test could not be reduced, because the input amplitudes were too small to produce significant perturbations in temperature.

4 POST-TEST ANALYSES

Both hand and analog studies were performed to explain the results of the inadvertent flow shutdown transient that occurred during the power test and to develop a model suitable for checking out revised emergency flow system controller designs. A revised pressure demand program was developed and shown to be adequate in providing sufficient flow to properly cool the tie rods during a flow shutdown.

A comparison was made between analog model pretest predictions and the NRX-A3 test data during the startup and the steady-state holds of the power test. The agreement was excellent during the startup ramps. At the holds, agreement was not as good because the actual temperature and flow demand profiles differed from the early test specification profiles which were used for the analog studies.

Extensive processing of wideband and Sanborn data from the NRX-A3 test series was performed, including component displacements, vibrations, torques, and strains; acoustic pressures; and also various temperatures, pressures, power levels, drum angles, etc., used in cross-correlation and sinusoidal transfer function measurements. To improve data accuracy and the methods for producing wideband data, the following operations were undertaken:

a) Several modifications to each of the digital computer codes were developed to improve the efficiency and flexibility of the wideband data processing system; and

b) The accuracy of the Test Cell "A" instrumentation system was determined and the dynamic response of pressure transducer impulse lines was computed analytically and confirmed by experiment.

Wideband data processing from the NRX-A3 test series has been completed. The SPIT, PLOT, and FORMAT codes developed at WANL, and the Huntsville Random Vibration Analysis Code were used extensively to process and analyze the data.

The SPIT code performs calibration, converts voltages into engineering units, and generates a magnetic tape for use as input to the PLOT and Huntsville format codes. The PLOT code prepares the data for presentation as SC-4020 PLOTS, whereas the Huntsville code is used to calculate power spectral densities and transfer functions.

BLANK PAGE

F. DISASSEMBLY AND POST-OPERATIONAL EXAMINATIONS

Disassembly of the NRX-A3 reactor assembly was initiated in the lower disassembly bay of the R-MAD Building on June 2, 1965, and continued until approximately July 2, 1965. The post-operational examinations of reactor components began on June 2, and were essentially complete at the time of this report. The post-operational examinations were performed primarily in the R-MAD lower and upper disassembly bay and the seven hot cells and junior cave associated with the R-MAD Building complex. Some examinations, primarily mechanical property examinations and metallography, were performed later at WANL, Large, or elsewhere.

A general evaluation, in summary form is given in the following paragraphs for the major components composing the NRX-A3 reactor assembly.

1 NON-NUCLEAR REACTOR COMPONENT EXAMINATION

The overall condition of all non-nuclear reactor components after disassembly was generally satisfactory. The majority of the components showed no visual evidence of test damage. Components which did exhibit damage are discussed below:

a) Control Drum Housing

The weld between the forward end of the bearing shaft and the control drum housing on drum No. 11 was observed to be separated. It is believed that the differential thermal expansions between the control drum housing and the beryllium cylinder produced sufficient stress to cause weld failure. Metallographic examination of the weld break showed that the weld was of good quality, but had only 0.020 inch to 0.025 inch penetration, rather than 0.030 inch as required by specifications. A stress analysis indicated that the membrane tensile stress in the weld exceeded the yield strength. It is, therefore, possible that the seven cryogenic cycles experienced by NRX-A3 would be sufficient to cause weld failure.

b) Filler Blocks

The band retaining lips on the aft ends of two filler blocks were found to be broken. An analysis indicates that these breaks could have occurred during the emergency shutdown at the end of EP-IV. The high temperature reached by the tie rods caused the core with the filler blocks to move aft toward the nozzle. The filler strips remain essentially stationary and could interfere with the filler blocks under such conditions.

c) Thermal Capsule Potting Compound

As in the NRX-A2, the thermal capsule potting material had suffered erosion and the capsules from several unfueled elements were lost. In addition the filler strip potting was severely attacked, permitting the capsules to fall out during disassembly. On NRX/EST, no potting is utilized in the core and the capsules are installed in close-fitting holes instead of the slots used in the NRX-A3.

d) O-Ring Seals

The O-rings which formed seals between the stainless steel tie rod liner tubes and the countersunk insulating sleeves were hardened and embrittled by the irradiation, and were generally broken in pieces during disassembly. This effect of irradiation had been anticipated in this temporary fix. O-ring seals are not planned for use in later reactors.

e) Support Blocks

Nearly all of the support blocks, except twelve which were fully coated with niobium, exhibited corrosion in the tie-rod hole. The sectioned fully-coated blocks, which contained coated tie-rod holes, showed no corrosion except for some small local spots beneath coating imperfections on the surface, caused by coating fixture removal during the manufacturing cycle. After being sectioned, most of the blocks revealed cracks that extended from the corner (fillet) radius of the aft counterbore, the face of which is a load-bearing surface, to the innermost flow holes. In several sectioned blocks, small corrosion cavities were observed in the crack area. Re-examination of the NRX-A2 blocks revealed that this same condition existed to a lesser degree. A comparison of NRX-A2 and NRX-A3 suggests that corrosion at this point is a result of these very fine cracks. The cracks are believed to be caused by the combined thermal and mechanical loads at the termination of a startup ramp.

There was also some evidence of external corrosion in very localized areas, but the overall condition of external surfaces and coating adherence was very good. One block was severely corroded in one lobe, but a re-check of pre-assembly inspection records indicated no coating, or extremely thin coating, in four holes of this lobe.

f) Insulating Cups

The condition of insulating cups was generally good, but on some, coating had flaked off. There was perhaps slightly more delamination present than before the test.

g) Tie-Rod Support Washers

The support washers in many cases sustained damage in the form of pitting, flaking, and corrosion at both inner and outer edges and flat faces. The attack was very irregular and unsymmetrical, and appears to be related to the cracking problem in the support block counterbore. There was no evidence of crushing of the washers. The adjacent insulating washers (also pyrographite) did not show significant damage, although light corrosion was observed in a few cases.

h) Central-Elements (Unfueled)

Unfueled central elements showed bore corrosion similar to that of NRX-A2, but more extensive. As in the NRX-A2, attack was irregular, and usually unsymmetrical with respect to the longitudinal axis. The nineteen central elements containing coated bores, were generally intact with little or no evidence of deterioration. In some instances the coating had deteriorared locally, exposing the graphite to mild surface attack.

Condition of the coated ends was generally good, but there was one notable exception in which local attack penetrated deeply into the external surfaces of a single-hole element.

Flexure-strength tests on sections of the unfueled elements showed good retention of strength, with an actual increase at the forward end, where radiation effects did not anneal out. One specimen, containing a pinhole, was positioned to be stressed in tension. The break occurred through the pinhole, with the reduction in strength of about 35 percent.

i) Insulating Sleeves

Soot deposits were observed on many insulating sleeves, which also contained some evidences of end corrosion or delamination. However, the general condition appeared to be good. Measurements of thermal conductivity of irradiated sleeves are in progress.

j) Liner Tubes

Approximately one-fourth of the stainless steel liner tubes in the core were examined in detail. Approximately 75 percent of those examined showed discoloration which was usually localized near joints in the insulating sleeves, and which were not present in the hotter, aft section. Similar discolorations were observed on NRX-A2 liner tubes. These discolorations are believed the result of migration of residual chlorides from the central unfueled element.

Approximately 50 percent of the liner tubes examined were damaged near the aft end by reaction (carbiding) with the pyrographite insulating sleeves. This condition was caused by the overheated condition which occurred during EP-IV.

k) Tie Rods

The appearance of the tie rods was, with minor exceptions, normal, although they had overheated near the aft end (by EP-IV shutdown). One tie rod showed discoloration around the underside of the button. Two contained a fused thermocouple near the button end of each tie rod.

Tensile tests on samples cut from the hot ends of tie rods revealed two samples with yield strengths of 64 and 93 ksi. These values compare with a range of values of 104 to 123 ksi obtained from samples cut from tie rods in colder regions of the core. It is presumed that other tie rods in the core were similarly affected, i.e., that full or partial annealing of a number of tie rods occurred during the emergency shutdown of EP-IV. However, none of the tie rods were found to be stretched, when compared with pre-operational measurements.

2 FUEL ELEMENT EXAMINATION

The results of post-operational examinations performed on the NRX-A3 fuel elements are summarized for the major interest areas based on the phenomena observed. These areas are:

1) Surface corrosion
2) Hot end corrosion
3) Channel exposure
4) Bore corrosion
5) Pinhole formation
6) Weight loss
7) Fuel bead behavior
8) Carbon deposits and bonding
9) Strength and dimensional changes
10) Behavior of peripheral elements

Information is also given on the behavior of the fuel elements with respect to various design fixes and of special types of fuel material present in the core. More detailed information on the performance of fuel elements and fuel element material is given in reference 49.

a) Surface Corrosion

Surface corrosion occurred in streak, edge, or patch patterns on 99.5 percent of the elements examined. The most predominant surface phenomena was one of streak (longitudinal) corrosion which occurred primarily at axial stations 19 to 23 with maximum occurrence at station 22. Typically, the effect was noted as parallel longitudinal streaks of surface corrosion between the underlying coolant channels. The streaks are believed to have originated from the high-temperature reaction of graphite with interstitial hydrogen. In some instances, streak corrosion produced channel exposure.

b) Hot End Corrosion

Corrosion was noted at the coated end of 90 percent of the fuel elements examined. Typically, this corrosion produced channel exposure (83.5 percent of the fuel elements examined). Visual evidence indicated that the major contributors to this effect were: (1) attack by hydrogen in areas of missing NbC end coatings and (2) leakage of hydrogen from the joint of the unfueled tips. While the widespread occurrence of corrosion at the hot end made it difficult to determine the exact number of leaking joints, unique point leakage effects were noted on 20.8 percent of the fuel elements examined. In general, corrosion and channel exposure at the hot end occurred on a higher fraction of the elements in the center region of the core than those at intermediate core radii or at the core periphery. The radial distribution of the average percent of end flats having channel exposure was 60 percent (5 cms), 43 percent (25 cms) and 20 percent (45 cms).

c) Channel Exposure

Exposure of one or more of the outer row of coolant channels occurred on 27.7 percent of the fuel elements examined. Visual examination data did not differentiate between exposure caused by surface corrosion or pinhole effects, but detailed examinations on a few elements indicated that both effects were contributing. Channel exposure occurred predominantly between axial stations 20 to 50 and ranged from less than an inch to several inches in length. The radial distribution indicated a higher percent of the elements in the center of the core (77 percent 5 cms) displayed the phenomena than those at the intermediate core radii (20 percent, 25 cms) or those at the core periphery (36 percent, 43 cms).

d) Bore Corrosion and Pinhole Information

Examination of the channels and microstructure in selected NRX-A3 elements indicated that bore corrosion was characterized by four distinct phenomena i.e.,

1) A punky substrate resulting from the preferential attack of graphite binder by hydrogen seeping through expansion cracks in the NbC liner. Corrosion of this type varied from element to element but occurred predominantly in two axial regions, stations 20-24 and 35-40 based on visual evidence, metallographic examination and incremental electrical resistance profiles.

2) Circumferential corrosion rings resulting from localized attack of the substrate through expansion cracks in the NbC liner. The severity and axial distributions of the effect varied from element to element. It was observed by visual examination to occur predominantly in two axial regions, stations 22 to 28 and 30 to 51.

3) A continuous gap between the liner and graphite substrate caused by general attack via a diffusion mechanism. This effect was intermingled with corrosion ring effects and varied in axial position and severity from element to element. It occurred predominantly from station 35 to the hot end. It should be noted that there was no evidence of bore corrosion effects occurring in the channels of the unfueled tips which were examined.

4) Relatively deep corrosion pockets, having no apparent circumferential symmetry. Corrosion pockets were observed on 29 percent of 89 axially slit fuel elements based on examination of 5 coolant channels per element. It appeared to be a random phenomena varying in axial occurrence from element to element. Pockets were observed from station 12 to 51 with maximum occurrence at station 38. Visual evidence indicated that two types of corrosion pockets occurred: (1) those associated with liner defects and (2) those associated with corrosion rings. Occasionally, corrosion pockets were observed to have resulted in interchannel communication or pinhole formation. The bore data obtained indicates that there was a general axial intermingling of the four types of bore corrosion. A possible explanation for this is that axial fuel element temperature distributions were significantly different during the high power holds (EP-IV and EP-V) and the medium power hold (EP-VI). Fuel element temperatures high enough to produce binder attack corrosion were obtained at downstream stations during the EP-VI test.

e) Pinhole Formation

A total of 3301 pinholes were observed on 928 fuel elements from the NRX-A3 core (58.2 percent of the elements examined). Pinholes were actually observed from station 2 to 51. The predominant occurrence was from station 30 to 51 with the maximum occurrence at station 38. The similarity between the axial distribution of corrosion pockets and pinholes and the visual examination results indicate that pinhole formation, at least in the maximum occurrence regions, is probably related to the formation of properly oriented corrosion pockets. However, pinholes form • the colder stations of the fuel elements are difficult to interpret in this respect. These may be due to a combination of corrosion pocketing, hydrogen pressure, flow distributions and surface corrosion effects. The radial distribution of the average percent pinholed elements was 70 percent (5 cms), 57 percent (25 cms) and 37 percent (43 cms). The radial distribution of pinhole severity (average number of pinholes per pinholed element) was 8 (2 cms), 3 (20 cms and 40 cms) and 6.6 (43 cms).

f) Element Weight Loss

Post weight measurements on 1096 fuel elements from NRX-A3 indicated an average weight loss per element of 10.6 grams. Although there was considerable scatter in the data, a general trend of decreasing weight loss with increasing core radius was observed. The radial distributions of the average weight loss per element was 15 grams (5 cms), 12 grams (25 cms), and 4.5 grams (43 cms). Summation of all of the weight data indicates a total weight loss of 11,608.5 grams for the 1,096 elements. Incremental resistance profiles, channel examination and incremental weight loss profile indicated that the axial regions of maximum weight loss due to bore corrosion were in the vicinity of station 20 and stations 35-40. The regions correspond to the axial areas of maximum binder attack (station 20) and maximum binder attack and/or bore corrosion (stations 36-40). Considering the difference in occurrence and severity between surface corrosion phenomena and bore corrosion phenomena observed in the NRX-A3 fuel elements, it is believed that the major contribution to the fuel element weight loss was made by bore corrosion, i.e., normal bore corrosion plus corrosion pockets and pinhole formation (reference 50). From an evaluation of all of the corrosion data, it is concluded that a significant portion of the weight loss occurred during the EP-VI test.

g) Fuel Bead Behavior

Metallographic examinations were performed on samples from 29 fuel elements at various axial stations. No evidence of fuel bead migration was observed which could be attributed to the effects of the reactor tests.

h) Carbon Deposits

Deposits tentatively identified as soot and pyrocarbon were observed on the surface of 92.5 percent of the fuel elements examined. The axial location of the deposits varied from element to element but in general, sooting was concentrated at stations 20 to 30 and pyrocarbon at stations 25 to 35. Visual evidence indicated that the deposits were probably related to the streak (longitudinal) corrosion occurring at stations upstream of the deposits. They were probably formed by the high temperature deposition of carbon from a saturated interstitial hydrogen gas phase.

Inter-element bonding was recorded for 160 elements in the NRX-A3 core. This bonding occurred predominantly in the region of carbon deposition at stations 25 to 35. A higher incidence of bonding was noted on elements near the core periphery although none of the peripheral elements were involved. It should be noted that the criteria for recording bonded elements was based on the degree of difficulty realized in separating them. Consequently, elements which may have been involved in weaker bonding were not recorded. In some cases bonded elements were broken during attempts to separate them. Metallographic examination of typically bonded interfaces indicated that the bonds were formed by carbon deposits filling the interelement gaps. The bonds were generally intermittent with regions of the interface not being bonded. These examinations indicated that pyrolytic carbon deposits were the probable cause for element bonding.

i) Strength and Dimensional Changes

One hundred ninety-one fuel samples from various axial locations in 29 fuel elements were flexure-tested at room temperature. The axial radial distribution of flexure strength obtained for the reactor-tested elements was compared with the pretest averages. These data indicated that the radiation effects and bore corrosion were the two factors predominantly influencing the strength changes observed.

Flexure strengths were observed to increase from 21 to 57 percent above the pretested average in the axial region 0 to 10 inches. In general, the increase in flexure strength in this region was highest in the peripheral elements and decreased in elements of decreasing core radius. Studies performed to determine the effect of thermal annealing on flexure strengths and incremental electrical resistance profiles indicated that the increase in strength in the 0-10 region was probably due to a radiation effect which appeared to be of varying magnitude with respect to the core radius.

Minimum flexure strengths were observed on the reactor elements at axial stations 20 to 25 and 35 to 45. The strength in these regions showed decreases varying from 10 to 35 percent below the pretest average. Again the magnitude of the decrease in strength appeared to be somewhat dependent on radial core positions although the dependency was not as pronounced as was observed for the cold and strength increases described above. It was concluded from these data, that the predominant factor causing the decrease in strength at these axial locations was that of bore corrosion.

The orificed length of 62 fuel elements was determined before and after the reactor test. A general decrease in length was observed which ranged from 15-25 mils for elements in the center region of the core to 2-7 mils for elements at the core periphery. The absence of corrosion at the exit faces of these elements and the temperature produced in the fuel during the reactor run indicate that the decreases are primarily due to graphitization effects produced during the high-power reactor runs (EP-IV and EP-V).

j) <u>Behavior of Peripheral Elements</u>

The peripheral elements in NRX-A3 were surface coated with NbC. In general, heavy surface corrosion (channel exposure), as noted in NRX-A2 on uncoated peripheral elements, did not exist on the regular 19 hole peripheral elements. The performance of the 12 hole, partial elements was significantly worse than the 19 hole peripheral elements. Significant amounts of edge corrosion and channel exposure occurred on the partial elements while the regular elements were essentially free of this effect. Corrosion and channel exposure at the hot end was significantly less on the coated peripheral elements, i.e., 89.3 percent of the non-peripheral elements and only 25.2 percent of the peripheral elements examined showed this effect. The improved performance of the regular NRX-A3 peripheral elements over that of the uncoated NRX-A2 peripheral elements (3) points to the significant role that the NbC coating plays in reducing surface corrosion phenomena in this critical area of the core (reference 51).

Element weight loss determinations were measured only on the regular, 19-hole elements. A significant drop in weight loss occurred in the peripheral elements of NRX-A3, i.e., an average of 4.5 grams per element for the peripheral elements as opposed to an average of 11.0 grams per element for non-peripheral elements.

Comparisons of pinhole occurrence on peripheral and non-peripheral fuel elements in NRX-A3 indicated that the NbC coatings did not inhibit pinhole formation. The fraction of peripheral elements which pinholed (37.1 percent) was not significantly different than the fraction of second row elements which pinholed (40 percent). However, pinhole severity (6.5) was higher than that observed on the second row elements (4.5).

1) Overcooled Vs. Normal Cooled Peripheral Fuel Element Performance

Overcooled elements showed less weight loss (4.8 gram average) than the normal-cooled elements (6.9 gram average). The most pronounced difference between these elements was in pinhole occurrence. Fifty percent of the overcooled elements had pinholed whereas none of the normal cooled elements displayed this effect. A slight reduction in surface corrosion effects was noted on second row elements adjacent to overcooled elements when compared to second row elements adjacent to the normal cooled elements. While heavy tile pattern corrosion effects as seen in NRX-A2 were not observed on the NRX-A3 peripheral elements, there was an indication of slightly higher surface corrosion effects on the second row elements as opposed to the third and fourth row elements.

2) Behavior of Elements Next to Pencil Seals

There was no marked reduction in surface corrosion on elements in the region of the pencil seals.

3) Behavior of Elements Graphitized in Helium at Y-12

A comparison was made between elements graphitized in helium at Y-12 and those graphitized in vacuum at Cheswick. Twenty-three elements, approximately at the same core radius were compared. These elements were all from the same coating batch. The elements graphitized in helium showed an average weight loss of 8.6 grams and 53 percent of them pinholed. The elements graphitized in vacuum had an average weight loss of 10 grams and 12 percent of them pinholed.

4) Behavior of Y-12 Elements

The behavior of the Y-12 elements in NRX-A3 was not significantly different than that of the Cheswick elements with respect to pinhole formation, surface corrosion and hot end corrosion effects. However, these elements in general showed a significantly higher weight loss when compared with Cheswick elements at the same core radius. The Y-12 elements had an average weight loss of about 16 grams per element, while the Cheswick elements had an average weight loss of 10 grams per element at a core radius of 35 cm.

V. BIBLIOGRAPHY

1) WANL-TNR-176, "NERVA Program NRX-A1 Test Final Report", September, 1964, CRD
2) WANL-TNR-193, "NERVA Program NRX-A2 Test Final Report", March, 1965, CRD
3) AGC-RN-S-0191, "Test Specifications for Cold Flow Development Test System", December, 1964, CRD
4) WANL-TME-1113, "NRX-A3 Reactivity Shimming Report", Reactor Analysis Department, March, 1965, CRD
5) WANL-TME-840A, "Reactor Analysis Data for NRX-A Reactors, Volume I", Reactor Analysis Department, March 15, 1965
6) WANL-TME-840A, "Reactor Analysis Data for NRX-A Reactors, Volume II", Reactor Analysis Department, March 15, 1965
7) WANL-TME-994, "Mechanical Design of the NRX-A3 Reactor", Reactor Design Department, November 1964, CRD
8) NTO-R-0030, "NRX-A3 Pretest Report", T. O. Harves, May 24, 1965
9) WANL-TNR-161, NRX-A3 Test Specification", Test Engineering, December 1964, CRD
10) WANL-TME-1053, "PAX Critical Experiments in Support of NRX-A3", Reactor Analysis Department, February 1965, CRD
11) WANL-TME-1125, "Core Exit Pressure Control System and Coupled Pressure Temperature Control System for NRX-A3", J. Josephson and C. C. Merchant, March 17, 1965
12) WANL-TNR-202, "Analysis of the NRX-A3 Test Series", Reactor Analysis Department, November 1965, CRD
13) WANL-TME-1050, "NRX-A3 Test Prediction Report", Reactor Analysis Department, January 1965, CRD
14) WANL-TME-1075, "NRX-A2 Post-Mortem Analysis", G. Downs, P. Stancampiano, P. Warner, January 1965
15) WANL-TME-1253, "NRX-A3 Post-Mortem Analysis", W. Persin and P. Stancampiano, August 1965, CRD
16) WANL-TME-1243, "NRX-A3 Post-Operative Mechanical Component Evaluation", D. W. Linde, September 1965, CRD
17) WANL-TME-1047, "WANL Calibrations for NRX-A3", T. C. Burlas, December 11, 1964

BIBLIOGRAPHY (CONT'D.)

18) WANL-TME-1099, "Stress Analysis: NRX-A3", A. G. Eggers, February 1965

19) WANL-TME-1071, "NRX-A2 Post-Operative Mechanical Component Evaluation", J. S. Karbowski

20) WANL-TME-979, "NRX-A2 Vibration Study Survey EML-55", G. M. Bove, September 1964

21) NTO-R-0036, "NRX-A3 Site Test Report", NERVA Test Operations, July 2, 1965

22) NTO-R-0040, "NRX-A3 Radiochemical Measurements", J. J. McCown, July 27, 1965 CRD

23) WANL-TME-1038, "Safety Evaluation Report - Part 2 NRX-A3 Reactor Test", Safeguards Engineering Division, January 1965, CRD

24) WANL-TNR-148, "Safety Analysis Report - NRX Testing", Safeguards Engineering Division, April 1964, CRD

25) WANL-TNR-165, "Radiation Analysis of NRX-A2 by Various Methods", M. A. Capo, December 7, 1964, CRD

26) WANL-TME-1195, "NRX-A3 Dosimetry Measurements (Part I and II)", F. H. Brooks, October 1965, CRD

27) WANL-TNR-199, "Analysis of NRX-A2 Reactor Test Results, Supplement 2", Reactor Analysis Department, July 1965, CRD

28) WANL-TME-804, "NRX-A2 Activation Analysis Report", L. D. Stephenson and J. Plainsek, August 1964, CRD

29) WANL-TME-530, "NRX-A1 and NRX-A2 Control System Final Report - CY 63", September 30, 1963

30) EGG 1183-1054, "Test Cell A Control Systems", Edgerton, Germeshausen, and Grier, Inc., Las Vegas, Nevada, June 1, 1964

31) WANL-TME-1083, "NRX-A2 Reactor Control Systems", C. C. Merchant and H. H. Norman, January 13, 1965

32) WANL-TME-1127, "Temperature Control System for NRX-A3", J. Josephson and D. Junker, March 13, 1965

33) LA(MS)3111, "Automatic Startup for Nuclear Reactors", G. L. Hohmann, B. G. Strait, August 1964

34) WANL-TME-1217, "Analysis of NRX-A3 Ambient GH_2 Flow Shutdown System", J. A. Rovnak and J. R. Lance, August 1965

35) WANL-TME-1123, "Analysis and Design of NRX-A3 Limiter Circuits", J. Josephson, March 12, 1965

BIBLIOGRAPHY (CONT' D.)

36) NTO-R-0026, "Three-Day Report for Experimental Plan II", April 20, 1965

37) NTO-R-0029, "Three-Day Report for Experimental Plan IIIA", May 18, 1965

38) NTO-R-0028, "Three-Day Report for Experimental Plan IV", April 28, 1965

39) WANL-TME-1270, "Analysis of PCV-41 Control System , K. Cooper and J. Josephson, October 1965

40) NTO-R-0035, "NRX-A3 Full Power Run EP-IV Anomalies", June 15, 1965

41) NTO-R-0032, "Three-Day Report for Experimental Plan VI", June 3, 1965

42) WANL-TME-1279, "Progress Report on High Temperature Thermocouples", W. F. Dunn, CRD

43) WANL-TME-1245, "NRX-A3 Instrumentation Disassembly and Post-Operative Report", E. K. Figenbaum, August 1965, CRD

44) WANL-TME-946, "Adequacy of TCA Instrumentation, Data Acquisition and Data Reduction Systems for NRX-A3 Testing", September 1964

45) NTO-R-0025, "Three-Day Report for Experimental Plan I", April 12, 1965

46) NTO-R-0031, "Three-Day Report Experimental Plan V", May 25, 1965

47) WANL-TME-1229, "Analysis of NRX-A3 EP-VI Control Test Results", J. Josephson and K. Cooper, September 1965

48) WANL-TME-12[illegible], "Transfer Function Measurements During the NRX-A3 Test Series", G. H. Steiner, C. A. Bodenschatz, and A. A. Wasserman, August 1965

49) WANL-TME-1333, "Post-Operational Evaluation of NRX-A3 Fuel Elements".

50) "The Hydrogen Corrosion Behavior of NERVA Fuel Elements", M. Blinn and G. Kilp, AIAA Propulsion Specialist Conference, 1965, Colorado Springs, Colorado, CRD

51) WANL-TME-1122, "Post-Operational Evaluation of NRX-A2 Fuel Elements", April 1965